ESTIMATES OF THE DIRECT AND INDIRECT RADIATIVE FORCING DUE TO TROPOSPHERIC AEROSOLS: A REVIEW

James Haywood
Meteorological Research Flight
U.K. Meteorological Office
Farnborough, England

Olivier Boucher[1]
Laboratoire d'Optique Atmosphérique
Université des Sciences et Technologies de Lille
Villeneuve d'Ascq, France

Abstract. This paper reviews the many developments in estimates of the direct and indirect global annual mean radiative forcing due to present-day concentrations of anthropogenic tropospheric aerosols since *Intergovernmental Panel on Climate Change* [1996]. The range of estimates of the global mean direct radiative forcing due to six distinct aerosol types is presented. Additionally, the indirect effect is split into two components corresponding to the radiative forcing due to modification of the radiative properties of clouds (cloud albedo effect) and the effects of anthropogenic aerosols upon the lifetime of clouds (cloud lifetime effect). The radiative forcing for anthropogenic sulphate aerosol ranges from -0.26 to -0.82 W m^{-2}. For fossil fuel black carbon the radiative forcing ranges from $+0.16$ W m^{-2} for an external mixture to $+0.42$ W m^{-2} for where the black carbon is modeled as internally mixed with sulphate aerosol. For fossil fuel organic carbon the two estimates of the likely weakest limit of the direct radiative forcing are -0.02 and -0.04 W m^{-2}. For biomass-burning sources of black carbon and organic carbon the combined radiative forcing ranges from -0.14 to -0.74 W m^{-2}. Estimates of the radiative forcing due to mineral dust vary widely from $+0.09$ to -0.46 W m^{-2}; even the sign of the radiative forcing is not well established due to the competing effects of solar and terrestrial radiative forcings. A single study provides a very tentative estimate of the radiative forcing of nitrates to be -0.03 W m^{-2}. Estimates of the cloud albedo indirect radiative forcing range from -0.3 to approximately -1.8 W m^{-2}. Although the cloud lifetime effect is identified as a potentially important climate forcing mechanism, it is difficult to quantify in the context of the present definition of radiative forcing of climate change and current model simulations. This is because its estimation by general circulation models necessarily includes some level of cloud and water vapor feedbacks, which affect the hydrological cycle and the dynamics of the atmosphere. Available models predict that the radiative flux perturbation associated with the cloud lifetime effect is of a magnitude similar to that of the cloud albedo effect.

1. INTRODUCTION

There has been much recent interest in the radiative effects of aerosols, particularly because anthropogenic activity is thought to have increased atmospheric concentrations. Atmospheric aerosols come from a wide variety of natural and anthropogenic sources and have typical radii ranging from 0.001 to 10 μm. Primary aerosols are emitted directly at the source, whereas secondary aerosols are generally formed from gaseous precursors by various gas and aqueous phase oxidation pathways. Primary aerosols include, for example, fly ash from industrial activities, sea-salt particles emitted at the ocean surface, or mineral dust aerosol that is emitted by the effects of wind erosion on arid land. An example of a secondary aerosol is sulphate aerosol that is formed from dimethyl sulphide (DMS) emissions by marine phytoplankton and from sulphur emissions from fossil fuel burning. Aerosols may undergo complex chemical reactions in the atmosphere and mix with each other either externally (where each particle contains a chemically distinct aerosol species) or internally (where each particle contains a combination of different aerosol species). Atmospheric aerosols are removed from the atmosphere either by impacting with the surface of the Earth (dry deposition) or by raining out in precipitating clouds (wet deposition). Typically, the lifetimes of aerosols in the troposphere range from a few minutes to several weeks. The geographically localized sources and sinks and relatively short atmospheric lifetimes give aerosols an extreme spatial and temporal inhomogeneity in the atmosphere. Tropospheric aerosols that are thought to have a substantial anthropogenic component include sulphate, black carbon, organic carbon, mineral dust, and nitrate aerosol. Anthropogenic aerosols influence the radiative budget of the Earth-atmosphere system in two different ways. The first is the direct effect, whereby aerosols scatter and absorb solar and thermal infrared

[1]On sabbatical leave at Abteilung Chemie der Atmosphäre, Max-Planck-Institut für Chemie, Mainz, Germany.

Reviews of Geophysics, 38, 4 / *November 2000*
pages 513–543
8755-1209/00/1999RG000078*$15.00*
Paper number 1999RG000078

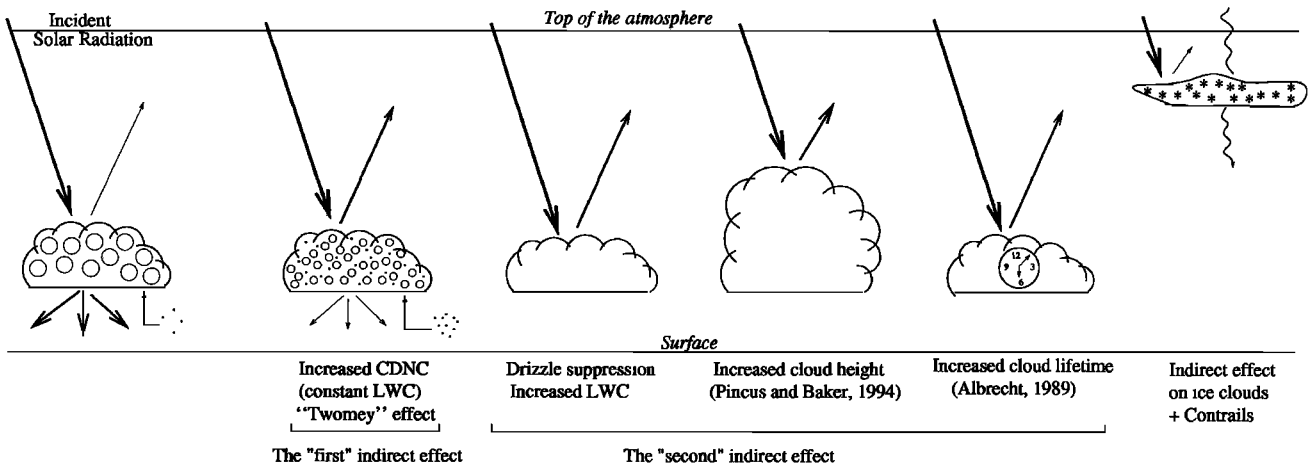

Figure 1. Schematic of the aerosol indirect effects. CDNC means cloud droplet number concentration, and LWC means liquid water content.

radiation, thereby altering the radiative balance of the Earth-atmosphere system or, equivalently, the planetary albedo. The second is the indirect effect, whereby aerosols modify the microphysical and hence the radiative properties and lifetime of clouds.

Radiative forcing is defined as the change in net irradiance at the tropopause due to an applied perturbation holding all atmospheric variables fixed, once stratospheric temperatures have been allowed to adjust to equilibrium. The concept of radiative forcing was first developed for one-dimensional (1-D) radiative convective models [e.g., *Manabe and Wetherald*, 1967; *Ramanathan and Coakley*, 1978; *Hansen et al.*, 1981], which investigated the change in the global mean surface air temperature at equilibrium, $dT_{\text{global mean}}$, due to the global mean radiative forcing $dF_{\text{adj global mean}}$ for radiatively active species. The relationship

$$dT_{\text{global mean}} = \lambda dF_{\text{adj global mean}},$$

where λ is the model-dependent climate sensitivity parameter, was found to be approximately independent of the forcing mechanism causing the radiative perturbation. Subsequent equilibrium model studies have extended the concept to 3-D models [e.g., *Cox et al.*, 1995; *Ramaswamy and Chen*, 1997; *Le Treut et al.*, 1998] and find that the relationship between $dT_{\text{global mean}}$ and $dF_{\text{adj global mean}}$ continues to hold to within an accuracy of ~20%. Stratospheric adjustment is important for atmospheric perturbations that change the temperature of the stratosphere and is particularly important for mechanisms such as stratospheric ozone depletion. For the majority of tropospheric aerosols the effects of stratospheric adjustment are likely to be insignificant, and stratospheric adjustment is often not accounted for. As the spatial and temporal variability of tropospheric aerosols is large, many studies report the global annual mean radiative forcing, which is a useful concept in determining the relative importance of perturbations of atmospheric species due to anthropogenic activity. This statement will be qualified when it comes to the aerosol indirect effect.

Intergovernmental Panel on Climate Change (*IPCC*) [1996] considered the direct radiative forcing from three different anthropogenic aerosol species: sulphate, fossil fuel black carbon (or soot), and biomass-burning aerosols. *IPCC* [1996] suggested a range of -0.2 to -0.8 W m^{-2} ("best guess" of -0.4 W m^{-2}) for sulphate aerosols, $+0.03$ to $+0.3$ W m^{-2} (best guess of $+0.1$ W m^{-2}) for fossil fuel black carbon aerosols, and -0.07 to -0.6 W m^{-2} (best guess of -0.2 W m^{-2}) for biomass-burning aerosols. The subjective confidence level of *IPCC* [1996] was "low" for sulphate aerosol and "very low" for fossil fuel black carbon and biomass-burning aerosol. Although best guess and confidence levels are presented by *IPCC* [1996], here we concentrate upon specific estimates available in the literature and present compilations of the ranges of estimates. This approach is taken because the validity of simply summing best guess estimates for the radiative forcing of each anthropogenic species to obtain an overall "best estimate" is very questionable. This is because different levels of uncertainty are associated with different aerosol species, because the ranges associated with each species make such a summation difficult, and because internal mixing complications lead to nonlinear absorption effects.

As is depicted in Figure 1, the aerosol indirect effect is usually split into two effects: the first indirect effect, whereby an increase in aerosols causes an increase in droplet concentration and a decrease in droplet size for fixed liquid water content [*Twomey*, 1974], and the second indirect effect, whereby the reduction in cloud droplet size affects the precipitation efficiency, tending to increase the liquid water content, the cloud lifetime [*Albrecht*, 1989], and the cloud thickness [*Pincus and Baker*, 1994]. The first and second indirect effects are also termed the "cloud albedo" and "cloud lifetime"

effects, respectively. Until recently, the first indirect effect has received much more attention than the second indirect effect. *IPCC* [1994] and *IPCC* [1996] only considered the cloud albedo effect. *Shine et al.* [1996] in the work of *IPCC* [1996] suggested a range of 0 to -1.5 W m^{-2} and no best guess value for the indirect radiative forcing. However, a value of -0.8 W m^{-2} was used for the year 1990 in the IS92a scenario by *Kattenberg et al.* [1996] in the work of *IPCC* [1996] and also *IPCC* [1999]. The confidence level for the indirect effect was classified as very low by *IPCC* [1996].

2. DIRECT RADIATIVE FORCING

Since *IPCC* [1996], there have been advances in both modeling and observational studies of the direct effect of tropospheric aerosols (see also the review by *Shine and Forster* [1999]). Global chemical transport modeling studies encompass a greater number of aerosol species and continue to improve the representation of the aerosol physical and chemical processes. The global models are more numerous and include more accurate radiative transfer codes, more sophisticated treatments of the effects of relative humidity for hygroscopic aerosols, better treatment of clouds, and better spatial and temporal resolution than some earlier studies. Additionally, dedicated field campaigns have been performed, and satellite retrieval methods for detecting the direct radiative effect of aerosols have been developed. The present-day direct radiative forcing due to aircraft emissions of sulphate and black carbon aerosol has been calculated to be insignificant [*IPCC*, 1999]. Section 2.1 provides an introduction to the methods used in determining the direct effect, and sections 2.2 and 2.3 consider sulphate and black and organic carbon aerosols. Section 2.4 investigates the radiative forcing due to anthropogenic mineral dust aerosol, and nitrates are briefly discussed in section 2.5. The complexities of treating internally mixed aerosols are discussed in section 2.6. Section 2.7 discusses field campaigns, and section 2.8 discusses developments in satellite retrievals. Section 2.9 discusses the uncertainties related to calculating the direct radiative forcing for aerosols.

2.1. Determining the Direct Radiative Forcing

Global mean calculations of the direct radiative forcing are made up of a series of local column calculations carried out either within a general circulation model (GCM) framework or off-line; thus it is useful to consider what factors determine the local radiative forcing at a particular geographic location. The optical properties of anthropogenic aerosols are described by three parameters: the extinction coefficient k_e, which determines the degree of interaction of radiation and the aerosol particles; the single scattering albedo ω_0, which determines the degree of absorption; and the scattering phase function, which determines the angular distribution of scattered radiation [e.g., *Kiehl and Briegleb*, 1993]. The scattering phase function may be integrated to provide parameters such as the asymmetry factor g, which is used in two-stream radiative transfer calculations, or the backscattered fraction β, which is used in more simple radiative transfer models [e.g., *Charlson et al.*, 1992]. These parameters are most frequently determined as a function of wavelength by assuming spherical particles and applying Mie scattering theory to a size distribution of aerosols with a specified refractive index. The local radiative forcing will depend upon the local atmospheric column burden of a particular anthropogenic aerosol species in the atmosphere, the underlying surface reflectance and the relative vertical position of the aerosol and cloud, the relative humidity if the aerosol is hygroscopic, and the insolation.

Figure 2 shows that partially absorbing aerosols (i.e., $\omega_0 \neq 1$) may exert a local negative forcing over regions with low surface reflectance and a positive forcing over regions of high surface reflectance [e.g., *Haywood and Shine*, 1995; *Chýlek and Wong*, 1995]. The boundary between local negative and positive solar forcing regimes is shown as a function of the single scattering albedo and surface reflectance for aerosols with differing backscattered fractions when clouds are excluded from the calculations. Similar results are found if partially absorbing aerosol resides above clouds that have a high albedo [e.g., *Haywood and Shine*, 1997]. It is not only the sign, but also the magnitude of the local radiative forcing, that is a function of the surface reflectance. Figure 3 shows idealized column calculations of the clear-sky radiative local forcing as a function of the solar zenith angle for scattering aerosol (Figure 3a) and absorbing aerosol (Figure 3b) [*Haywood and Shine*, 1997]. The clear-sky local radiative forcing due to scattering aerosol is a function of the solar zenith angle, showing a maximum radiative forcing at solar zenith angles of between 60° and 80° due to the nature of the scattering phase function of the aerosol [e.g., *Pilinis et al.*, 1995; *Nemesure et al.*, 1995; *Boucher et al.*, 1998]. The radiative forcing is also a function of the surface reflectance, showing the strongest radiative forcing when the surface reflectance is low. For the absorbing aerosol the strongest radiative forcing occurs when the surface reflectance is high.

The global annual mean radiative forcing of a particular anthropogenic aerosol is determined by its temporal and spatial distribution in the atmosphere together with its optical properties. The atmospheric burden is determined by emission processes, chemical reactions, and deposition and transport processes, each of which must be accurately modeled by global chemical transport models [e.g., *Langner and Rodhe*, 1991; *Pham et al.*, 1995; *Penner et al.*, 1998]. The optical properties of aerosols may depend upon the three-dimensional geographic distribution of the aerosols. For example, in conditions of high relative humidity, hygroscopic aerosols take up water, leading to changes in chemical composition and size of the aerosol particles and hence

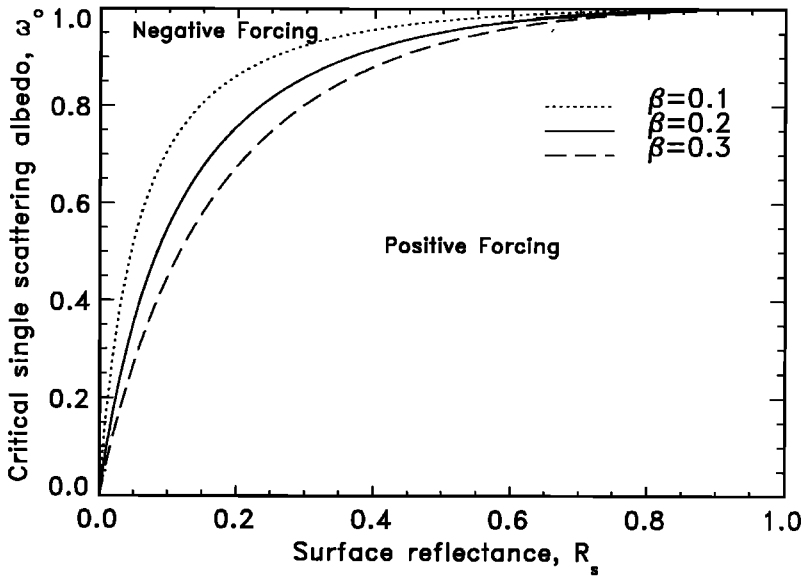

Figure 2. The critical single scattering albedo ω_0, at which the clear-sky radiative forcing changes sign as a function of surface reflectance R_s, for different backscattered fractions β (adapted from *Haywood and Shine* [1995]).

variations in the optical parameters. The global annual mean radiative forcing is also dependent upon the three-dimensional distribution in the atmosphere because the radiative forcing depends upon spatially dependent fields such as insolation, cloud amount, and underlying surface reflectance. In 3-D modeling studies of the direct effect discussed here, it is important to realize that the radiative forcing is calculated in a purely diagnostic way. Radiative calculations are performed excluding and including the aerosol perturbation, and the difference in the net radiation at the tropopause yields the radiative forcing. In GCM calculations the effect of the aerosols upon the atmospheric heating rates is not included in the dynamical evolution of the atmosphere, and thus no feedback mechanisms are included. We now concentrate upon estimates of the global annual mean radiative forcing estimates for specific species.

2.2. Sulphate Aerosol

The main source of anthropogenic sulphate aerosol is via sulphur dioxide emissions from fossil fuel burning, with a relatively small contribution from biomass burning. The main natural sources of sulphate aerosol are from DMS emissions and volcanoes. Estimates of the

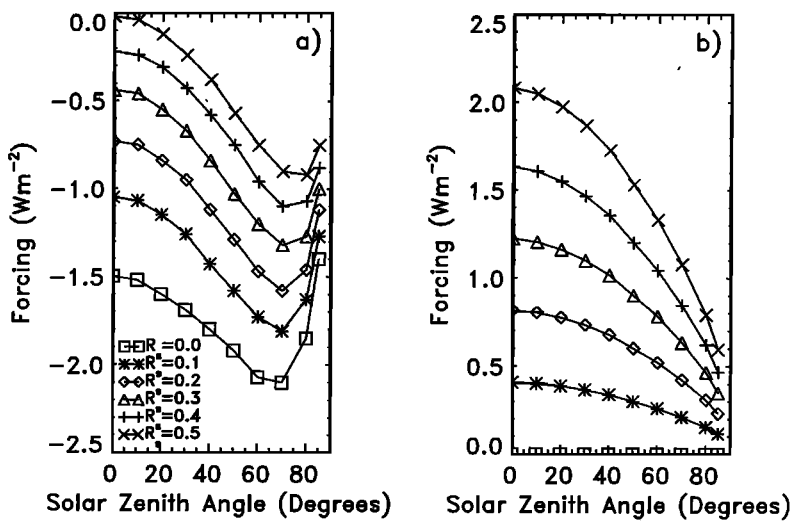

Figure 3. Examples of column calculations of the clear-sky radiative forcing for (a) scattering aerosol (sulphate) and (b) absorbing aerosol (black carbon) as a function of solar zenith angle for different Lambertian surface reflectances, R_s (adapted from *Haywood and Shine* [1997]). Reprinted with permission from The Royal Meteorological Society.

global emissions of sulphate aerosol from anthropogenic and natural sources are given in Table 1. Estimates of the current magnitude and geographic distribution of emissions of sulphur from fossil fuels are fairly well known because inventories of fossil fuel burning are available [e.g., *Benkovitz et al.*, 1996]. Global mean emissions used in recent chemical transport modeling of the sulphur cycle range from 66.8 to 92.4 Tg S yr^{-1} for anthropogenic emissions and from 91.7 to 125.5 Tg S yr^{-1} for total emissions. The main oxidation pathways that transform sulphur dioxide into sulphate aerosols are via gaseous phase reactions with the hydroxyl radical and aqueous phase reactions within cloud droplets [e.g., *Pham et al.*, 1995]. These reactions are parameterized in chemical transport models (CTMs) together with dry and wet deposition processes. While these parameterizations are physically based wherever possible, uncertainties in the input parameters lead to differences in the atmospheric burdens of sulphate aerosol; the burdens of total and anthropogenic sulphate from different models are shown in Table 1.

Having briefly discussed the results from CTMs, we now focus on estimates of the direct radiative forcing. Early 1-D box-model estimates of the radiative forcing [e.g., *Charlson et al.*, 1992] using simplified expressions for radiative forcing have been superseded by global calculations using prescribed aerosol concentrations from CTMs. These studies use either 3-D observed fields of, for example, clouds, relative humidity, and surface reflectance [e.g., *Kiehl and Briegleb*, 1993; *Myhre et al.*, 1998], or GCM-generated fields [e.g., *Boucher and Anderson*, 1995; *Haywood et al.*, 1997a] together with the prescribed aerosol distributions from CTMs and detailed radiative transfer codes in calculating the radiative forcing. A growing number of studies perform both the chemical transportation of aerosols and the radiative forcing calculations, which have the advantage of correlating predicted aerosol distributions precisely with fields determining aerosol production and deposition such as clouds [e.g., *Penner et al.*, 1998]. Table 2 summarizes estimates of the radiative forcing due to sulphate from global modeling studies.

The global mean radiative forcing ranges from −0.26 to −0.82 W m^{-2}, although most lie in the range −0.26 to −0.4 W m^{-2}. The spatial distribution of the forcings is similar in all of the studies, an example of which is shown in Plate 1a [*Haywood et al.*, 1997a]. The radiative forcing is negative everywhere and is strongest over industrial regions of the Northern Hemisphere, although the ratio of the annual mean Northern Hemisphere/Southern Hemisphere radiative forcing varies from 2.0 [*Graf et al.*, 1997] to 8.7 [*Koch et al.*, 1999]. The ratio of the annual mean radiative forcing over land to that over ocean also varies considerably, ranging from 1.3 [*Kiehl et al.*, 2000] to 3.4 [*Boucher and Anderson*, 1995]. The seasonal cycle is strongest in the Northern Hemisphere summer when the insolation is the highest, although different seasonal cycles of the sulphate burden from the chemical trans-

TABLE 1. Estimates of the Global Present-Day Emissions of Various Different Types of Aerosol From Various Sources

Emission	*Source*	*Langner and Rodhe [1991]*	*Pham et al. [1995]*	*Chin and Jacob [1996]*	*Chuang et al. [1997]*	*Feichter et al. [1997]*	*van Dorland et al. [1997]*	*Graf et al. [1997]*	*Restad et al. [1998]*	*Koch et al. [1999]*	*Lohmann et al. [1999b]*
SO_2, Tg S yr^{-1}	anthropogenic	70.0	92.4	67.4	75.7	66.8	74	78	65	66.6	66.8
	biomass burning	2.5	3.0	NA	2.2	2.5	2	2	2	2.3	2.5
	volcanic	8.5	9.2	6.7	3.4	8.0	6	14	8.7	3.5	8.0
	oceanic	16.0	19.7	22.6	23.7	18.1	16	25	16	10.7	17.5
	other	1.0	1.2	0	1.0	0.9	NA	NA	NA	0.1	0.9
	total	98.0	125.5	96.7	106.0	96.3	98	119	91.7	83.2	95.7
Atmospheric burden, Tg SO_4	total	2.31 (1.56s)[a]	2.4	1.59	1.65	2.04	NA	2.34	1.51	2.19	3.09
	anthropogenic	1.18 (0.90s)	1.65	0.60	1.07	1.14	1.08	0.87	0.97	1.68	NA

Emission	*Source*	*Ghan and Penner [1992]*	*Cooke and Wilson [1996]*	*Liousse et al. [1996]*	*Cooke et al. [1999]*	*Penner et al. [1993]*
Black carbon, Tg C yr^{-1}	fossil fuel	5.8	8.0	6.6	6.4	6.6
	biomass burning	NA	6.0	12.3	NA	17.2
Organic carbon, Tg C yr^{-1}	fossil fuel	NA	NA	20.4	10.1	NA
	biomass burning	NA	NA	31.9	NA	NA

NA means not accounted for or not available.
[a]In Tables 1 and 2, appended "s" indicates the slow oxidation case rather than the standard oxidation case.

TABLE 2. The Global-Mean Annual-Average Direct Radiative Forcing Due to Sulphate Aerosols From Different Global Studies

Study	ω_0 (0.55 μm)	$k_{e,}$ $m^2 g^{-1}$ SO_4 (0.55 μm)	g (0.55 μm)	Direct Radiative Forcing, $W m^{-2}$	Anthropogenic Column Burden, $mg m^{-2}$	Normalized Radiative Forcing, $W g^{-1}$	Cloud Scheme	Direct Radiative Forcing		Source of Sulphate Data
								NH/SH	Land/Ocean	
Boucher and Anderson [1995]	1.0	3.12	0.60	−0.29	2.32	−125	frac	4.3	3.4	*Langner and Rodhe* [1991]
Graf et al. [1997]	NA	NA	NA	−0.26	1.70	−153	frac	2.0	NA	*Graf et al.* [1997]
Feichter et al. [1997]	<1.0	5.0	NA	−0.35	2.23	−157	frac	4.2	1.4	*Feichter et al.* [1997]
Kiehl and Briegleb [1993]	1.0	5.0	0.69	−0.28	1.76	−159	frac	3.3	NA	*Langner and Rodhe* [1991]s
Myhre et al. [1998]	1.0	5.0	0.64	−0.32	1.90	−169	frac	6.9	NA	*Restad et al.* [1998]
van Dorland et al. [1997]	<1.0	4.0	NA	−0.36	2.11	−171	frac	5.0	NA	*van Dorland et al.* [1997]
Koch et al. [1999]	1.0	5.0	NA	−0.68	3.3	−200	frac	8.7	NA	*Koch et al.* [1999]
Kiehl and Rodhe [1995]	1.0	5.0	0.69	−0.66	3.23	−204	frac	NA	NA	*Pham et al.* [1995]
				−0.29	1.76	−165	frac	NA	NA	*Langner and Rodhe* [1991]s
Chuang et al. [1997]	1.0	5.0	0.64	−0.43	2.10	−205	on/off[a]	4.7	2.4	*Chuang et al.* [1997]
Haywood et al. [1997a]	1.0	5.0	0.64	−0.38	1.76	−215	frac	4.0	NA	*Langner and Rodhe* [1991]s
Hansen et al. [1998]	1.0	NA	NA	−0.28	1.14	−246	frac	NA	NA	*Chin and Jacob* [1996]
Kiehl et al. [2000]	1.0	5.0	0.66	−0.56	2.23	−251	frac	2.7	1.3	*Barth et al.* [2000]
Haywood and Ramaswamy [1998]	1.0	5.0	0.64	−0.63	1.76	−358	on/off	3.6	2.6	*Langner and Rodhe* [1991]s
				−0.82	1.76	−460	on/off	5.8	2.7	*Kasibhatla et al.* [1997]
Penner et al. [1998] and *Grant et al.* [1999]	1.0	5.07	0.65	−0.81	1.82	−445	on/off	4.5	2.3	*Penner et al.* [1998]

The optical parameters for sulphate aerosol at 0% relative humidity at a wavelength of 0.55 μm are shown. The anthropogenic column burden of sulphate and the source of the sulphate data are shown together with the normalized radiative forcing. "Frac" indicates a cloud scheme with fractional grid box cloud amount, and "on/off" indicates that a grid box becomes totally cloudy once a certain relative humidity threshold is reached. The ratio of the Northern Hemisphere direct radiative forcing to the Southern Hemisphere direct radiative forcing and the ratio of the mean radiative forcing over land to the mean radiative forcing over oceans are also shown. NA means that data are not available. LR91s indicates that the slow oxidation case was used in the calculations.

[a]The maximum hygroscopic growth of the aerosols was restricted to a relative humidity of 90%.

port models result in maximum global mean radiative forcings ranging from May to August [e.g., *Haywood and Ramaswamy*, 1998]. The ratio of the June-July-August/December-January-February (JJA/DJF) radiative forcing is estimated to lie in the range from less than 2 [*van Dorland et al.*, 1997] to more than 5 [*Grant et al.*, 1999]. The range in the normalized radiative forcing (i.e., the radiative forcing per unit mass of sulphate aerosol as defined by *Nemesure et al.* [1995] or *Pilinis et al.* [1995]) accounts for different anthropogenic loadings from the chemical transport models and is similar to the uncertainty in the total radiative forcing. This indicates that differences in the radiative forcing are not due solely to different mass loadings from the CTMs. The optical parameters for sulphate aerosol in each of the studies may vary. Although the single scattering albedo of pure sulphate is close to unity, some of the studies [e.g., *van Dorland et al.*, 1997; *Feichter et al.*, 1997] include some absorption. *Charlson et al.* [1999] shows considerable variation in the specific extinction coefficient used in different studies, particularly when accounting for relative humidity effects. The treatment of the effects of relative humidity and cloud appear to be particularly important in determining the radiative forcing. The studies of *Haywood and Ramaswamy* [1998], *Penner et al.* [1998], and *Grant et al.* [1999] produce normalized radiative forcings a factor of 2–3 higher than the other studies. Both *Haywood and Ramaswamy* [1998] and *Penner et al.* [1998] acknowledge that their use of on/off cloud schemes where cloud fills an entire grid box once a threshold relative humidity is exceeded may lead to strong radiative forcings due to strong nonlinear relative humidity effects. *Chuang et al.* [1997] use an on/off cloud scheme and report a radiative forcing lower than these two studies, but the hygroscopic growth is suppressed above a relative humidity of 90%. The use of monthly-mean relative humidity fields in some of the calculations [e.g., *Kiehl and Briegleb*, 1993; *Myhre et al.*, 1998] leads to lower radiative forcings, as temporal variations in relative humidity and associated nonlinear effects are not accounted for. *Kiehl et al.* [2000] improve the treatment of relative humidity compared with *Kiehl and Briegleb* [1993] and *Kiehl and Rodhe* [1995] by improving the relative humidity dependence of the aerosol optical properties and by using on-line GCM relative humidities rather than monthly mean analyses, resulting in a larger normalized radiative forcing. *Haywood and Ramaswamy*'s [1998] GCM study indicates a stronger radiative forcing when sulphate resides near the surface because the relative humidity is higher. GCM sensitivity studies [*Boucher and Anderson*, 1995] and column calculations [*Nemesure et al.*, 1995] show that the radiative forcing is a strong function of relative humidity but relatively insensitive to chemical composition. The contribution to the global forcing from cloudy regions is predicted to be 4% [*Haywood et al.*, 1997a], 11% [*Haywood and Ramaswamy*, 1998], 22% [*Boucher and Anderson*, 1995], and 27% [*Myhre et al.*, 1998] and hence remains uncertain. Studies that impose clear skies [e.g., *Schult et al.*, 1997; *Kirkevåg et al.*, 1999] obtain radiative forcings much stronger than those using observed or modeled cloud distributions. The global mean longwave radiative forcing has been estimated to be less than $+0.01$ W m^{-2} and is insignificant [*Haywood et al.*, 1997a].

Boucher and Anderson [1995] investigate the effects of different size distributions, finding a 20–30% variation in the radiative forcing for reasonable accumulation-mode size distributions. *Nemesure et al.* [1995] and *Boucher et al.* [1998] find a much larger sensitivity to the assumed size distribution, as sulphate is modeled by much narrower size distributions. Column radiative forcing calculations by 15 radiative transfer codes of varying complexity [*Boucher et al.*, 1998] show that for well-constrained input data, differences in the computed radiative forcing when clouds are excluded are relatively modest at approximately $\pm 20\%$ (Figure 4). This indicates that uncertainties in the input parameters and in the implementation of the radiative transfer codes and the inclusion of clouds lead to the large spread in estimates, as suggested by *Penner et al.* [1994].

Additional column calculations show a weakened radiative forcing when the cloud optical depth is much greater than the aerosol optical depth [*Haywood and Shine*, 1997; *Liao and Seinfeld*, 1998] and that the forcing is insensitive to the relative vertical position of the cloud and aerosol. *Haywood et al.* [1997b, 1998] used a cloud-resolving model and investigated effects of subgrid-scale variations in relative humidity and cloud. For their case study the optical depth and radiative forcing in a GCM-sized grid box were underestimated by 60%. *Ghan and Easter* [1998] came to similar conclusions. Effects of subgrid-scale variations in relative humidity and cloud on a global scale have not been rigorously investigated.

2.3. Black Carbon and Organic Carbon

Measurements show that atmospheric black carbon (BC) and organic carbon (OC) aerosol particles frequently contribute significantly to the total aerosol mass [e.g., *Novakov et al.*, 1997]. BC is emitted as primary particles from incomplete combustion processes, such as fossil fuel and biomass burning, and therefore much atmospheric BC is of anthropogenic origin. Naturally occurring biomass fires do occur, but the quantity of BC emitted from these nonanthropogenic sources is very difficult to quantify. OC is emitted as both primary particles and by secondary production from gaseous compounds via condensation or gas phase oxidation of hydrocarbons. Primary organic aerosols come from both anthropogenic sources (fossil fuel and biomass burning) and from natural sources (such as debris, pollen, spores, and algae). Detailed emission inventories for both BC and OC have recently been developed [e.g., *Penner et al.*, 1993; *Cooke and Wilson*, 1996; *Liousse et al.*, 1996; *Cooke et al.*, 1999] that consider both fossil fuel and biomass components (see Table 1). The inventories of biomass-

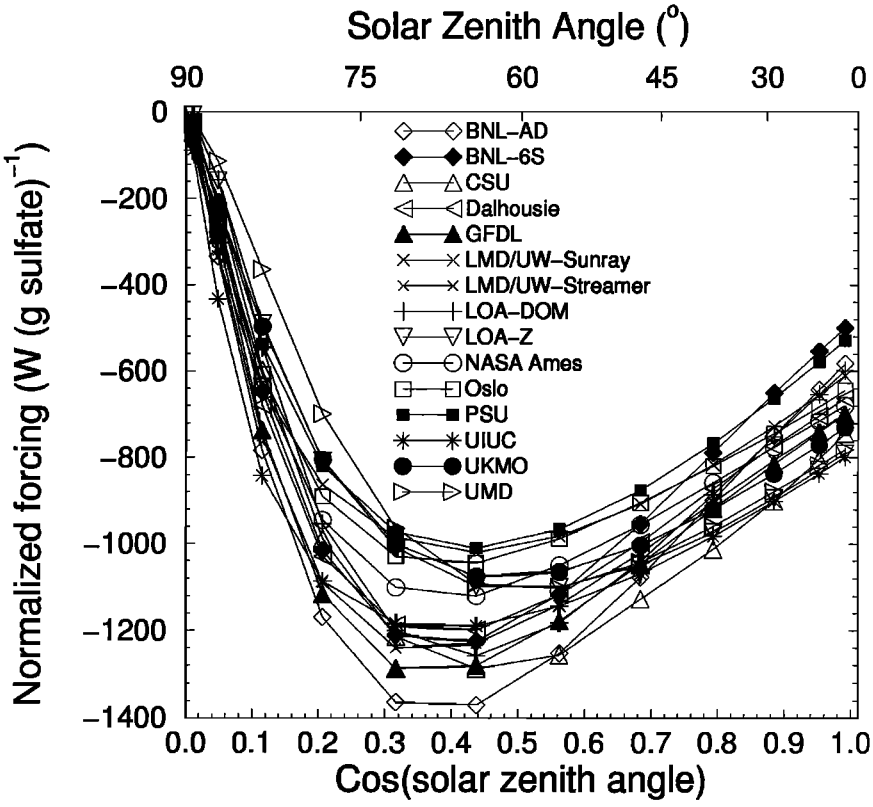

Figure 4. The normalized clear-sky radiative forcing for sulphate aerosol from the intercomparison study of *Boucher et al.* [1998]. A lognormal distribution with a geometric mean diameter of 0.170 μm and a geometric standard deviation of 1.105, together with an aerosol optical depth of 0.20 at 0.55 μm and a Lambertian surface reflectance of 0.15, were assumed. For details of the radiation codes used in the calculations, see *Boucher et al.* [1998].

burning BC and OC particles are more difficult to constrain than fossil fuel emissions, owing to the paucity of data. OC emissions are particularly difficult to constrain because measurements of OC are particularly difficult to make and often include a substantial natural component and because of secondary production. Currently, the complex reactions that form secondary organic aerosol are not included explicitly in model estimates of the OC burden and the subsequent radiative forcing [e.g., *Cooke et al.*, 1999; *Penner et al.*, 1998]. *Cooke et al.* [1999] attempt to account for these important processes by multiplying the burden of primary OC by a factor of 2, while *Penner et al.* [1998] account for the formation of secondary OC particles in the construction of the emission inventories [*Liousse et al.*, 1996].

Since *IPCC* [1996], there have been a number of more refined 3-D global model estimates of the radiative forcing due to BC aerosol from fossil fuel burning that have superseded calculations using simple expressions for the radiative forcing [e.g., *Haywood and Shine*, 1995; *Chýlek and Wong*, 1995] where the contribution from cloudy regions was not included. These estimates now include the contribution to the total radiative forcing from areas where BC exists either above or within clouds, although the treatment of BC within clouds remains crude. There are two main sources of black carbon aerosol: fossil fuel and biomass burning. The radiative forcing due to fossil fuel BC is considered in section 2.3.1, and the radiative forcing due to fossil fuel OC is considered in section 2.3.2. Section 2.3.3 considers the radiative forcing due to OC and BC from biomass emissions, and section 2.3.4 considers other studies that have examined OC and/or BC. Table 3 summarizes recent global annual-mean estimates of the radiative forcing due to BC and OC aerosol from recent studies.

2.3.1. Fossil fuel BC. The radiative forcing of fossil fuel BC has received considerable attention. *Haywood et al.* [1997a] and *Myhre et al.* [1998] assumed that fossil fuel BC was directly proportional to the mass of sulphate from *Langner and Rodhe* [1991] and *Restad et al.* [1998], respectively, by applying a 7.5% mass scaling (equivalent to a global mean burden of approximately 0.13 to 0.14 mg m^{-2}). Global annual-mean radiative forcings of +0.20 and +0.16 W m^{-2} are calculated for external mixtures from the respective studies. If BC were modeled as an internal mixture with sulphate aerosol, *Haywood et al.* [1997a] and *Myhre et al.* [1998] suggest that the degree of absorption may be considerably enhanced and the radiative forcing strengthens to +0.36 and +0.44 W m^{-2}, respectively. These estimates were performed

TABLE 3. The Global-Mean Annual-Average Direct Radiative Forcing Due to Black Carbon and Organic Carbon Aerosols From Different Studies

Aerosol	*Author*	*Mixing or Optical Parameters*	ω_0	k_e, $m^2 g^{-1}$	*Direct Radiative Forcing, W m^{-2}*	*Column Burden, mg m^{-2}*	*Normalized Radiative Forcing, W g^{-1}*	*Remarks*
Fossil fuel BC	*Haywood et al.* [1997a]	external	0.21	9.3	+0.20	0.13	1525	GCM study; 7.5% mass scaling of BC to SO_4 assumed; SO_4 from *Langner and Rodhe* [1991] (slow oxidation case); λ = 0.55 μm, RH = inv
		internal with sulphate	0.91	11.1	+0.36	0.13	2770	internal mixing approximated by volume weighting the refractive indices of BC and SO_4; λ = 0.55 μm, RH = 80%
	Myhre et al. [1998]	external	0.21	9.3	+0.16	0.14	1123	three-dimensional study using global climatologies for cloud, surface reflectance, etc.; 7.5% mass scaling of BC to SO_4 assumed; SO_4 from *Restad et al.* [1998]; λ = 0.55 μm, RH = inv
		internal with sulphate	0.77	5.5	+0.42	0.14	3000	internal mixing approximated by volume weighting the refractive indices of BC and SO_4; λ = 0.55 μm, RH = 0%
	Penner et al. [1998] and *Grant et al.* [1999]	internal	NA	NA	+0.20	0.16	1287	BC modeled using chemical transport model and GCM; BC and OC fractions vary geographically
	Cooke et al. [1999]	external	0.23	11.0	+0.17	0.14	1210	BC modeled using chemical transport model and GCM; λ = 0.50 μm, RH = inv
	Haywood and Ramaswamy [1998]	external mixture	0.21	9.3	+0.2	0.13	1500	three-dimensional GCM study using *Cooke and Wilson* [1996] BC data scaled to *Liousse et al.* [1996] total BC mass; 50% of the BC mass assumed to be from fossil fuels; λ = 0.55 μm, RH = inv
Fossil fuel OC	*Penner et al.* [1998]	internal with fossil fuel BC	1.0	5.3	−0.04	~0.7	−60	OC modeled using chemical transport model and GCM; may be more negative due to mixing and effects of RH; 0.5–0.69 μm, RH = 0%
	Cooke et al. [1999]	external mixture	0.98	3.6	−0.02	0.34	−70	OC modeled using chemical transport model and GCM; may be more negative due to effects of RH and assumption of partial absorption of OC; λ = 0.5 μm, RH = inv
Biomass burning (BC + OC)	*Hobbs et al.* [1997]	optical parameters of biomass smoke	0.88	4.3	−0.3	3.7	−80	uses simplified expression from *Chylek and Wong* [1995]; neglects radiative forcing from cloudy areas; other parameters including estimated column burden from *Penner et al.* [1992]; λ = 0.55 μm, RH = 80%
	Iacobellis et al. [1999]	optical parameters of biomass smoke	0.97	9.06	−0.74	3.5	−210	three-dimensional chemical transport model and GCM; simplified expressions also examined; λ = 0.25–0.68 μm, RH = 0%
	Penner et al. [1998] and *Grant et al.* [1999]	internal mixture of OC and BC	0.98	2.4	−0.14 to −0.21	1.76	−80 to −120	three-dimensional chemical transport model and GCM using biomass optical parameters modeled from two observational studies; λ = 0.5–0.69 μm, RH = 0%
Fossil fuel and biomass-burning BC	*Haywood and Ramaswamy* [1998]	external mixture	0.21	9.3	+0.4	0.27	1500	three-dimensional GCM study using *Cooke and Wilson* [1996] BC data scaled to *Liousse et al.* [1996] total BC mass; λ = 0.55 μm, RH = inv
Fossil fuel and biomass-burning BC	*Hansen et al.* [1998]	observed ω_0	NA	NA	+0.27	NA	NA	adjustment of modeled single scattering albedo from 1.0 to 0.92–0.95 to account for the absorption properties of BC
Fossil fuel and biomass-burning OC	*Hansen et al.* [1998]	external mixture	1.0	NA	−0.41	NA	NA	three-dimensional GCM study using *Liousse et al.* [1996] OC data; OC modeled as scattering aerosols; λ = 0.55, RH = inv

The type of mixing or source of optical parameters is shown. The single scattering albedo ω_0 and the specific extinction coefficient k_e are shown together with the wavelength λ and the relative humidity (RH). "Inv" indicates that the optical parameters are invariant with relative humidity. The anthropogenic column burdens of black carbon (BC) and organic carbon (OC) are shown together with the normalized direct radiative forcing. GCM means general circulation model.

before global modeling studies for BC were generally available. *Haywood and Ramaswamy* [1998] rescaled the global column burden of BC from *Cooke and Wilson* [1996] to that of *Liousse et al.* [1996], which is thought to be more representative of optically active BC, and estimated the radiative forcing due to fossil fuel and biomass burning to be approximately +0.4 W m^{-2}. Approximately half of the radiative forcing due to BC was attributed to fossil fuel burning sources, leading to a fossil fuel BC radiative forcing of +0.2 W m^{-2}. *Penner et al.* [1998] and *Grant et al.* [1999] used a chemical transport model in conjunction with a GCM to estimate a global column burden of BC from fossil fuel emissions of 0.16 mg m^{-2} and a radiative forcing of +0.20 W m^{-2}. *Cooke et al.* [1999] estimated the global burden of optically active BC aerosol from fossil fuel burning from a 1° × 1° inventory of emissions to be 0.14 mg m^{-2} and a subsequent radiative forcing of +0.18 W m^{-2}. The good agreement of the assumed column burdens of *Haywood et al.* [1997a] and *Myhre et al.* [1998] should be noted. *Grant et al.* [1999] suggest that the global mean radiative forcing due to fossil fuel BC is strongest in JJA owing to the larger insolation coupled with higher atmospheric concentrations in the Northern Hemisphere. The normalized radiative forcing due to an external mixture of BC appears reasonably consistent throughout the studies, ranging from +1123 to +1525 W g^{-1}. However, all these studies used the same size distribution and exclude effects of relative humidity, and thus the modeled specific extinction is independent of the relative humidity at approximately 10 m^2 g^{-1} at 0.55 μm. Observational studies show a wide range of specific extinction coefficients [e.g., *Liousse et al.*, 1993; *Horvath*, 1993; *Martins et al.*, 1998] of approximately 5–20 m^2 g^{-1} at 0.55 μm, and thus the uncertainty in the associated radiative forcing is likely to be higher than the global model results suggest. Additionally, if BC were modeled as an internal mixture, *Haywood et al.* [1997a] and *Myhre et al.* [1998] suggest the degree of absorption may be considerably enhanced, the radiative forcing being estimated as +0.36 and +0.44 W m^{-2}, respectively. Both of these studies use relatively simple effective medium mixing rules for determining the composite refractive index of internally mixed BC with sulphate and water. Detailed scattering studies including a randomly positioned black carbon sphere in a scattering droplet show that the absorption is relatively well represented by effective medium approximations [*Chýlek et al.*, 1996b]. Column studies by *Haywood and Shine* [1997] and *Liao and Seinfeld* [1998] and the global studies by *Haywood and Ramaswamy* [1998] and *Penner et al.* [1998] suggest that the radiative forcing due to BC will be enhanced if BC exists above the cloud but will be reduced if the BC is below the cloud; thus the vertical profile of BC aerosol must be modeled accurately.

2.3.2. Fossil fuel OC. The radiative forcing due to fossil fuel OC has been investigated by *Penner et al.* [1998] and *Grant et al.* [1999]. They modeled the radiative forcing due to an internal mixture of fossil fuel BC and OC and found that the radiative forcing weakened from +0.20 W m^{-2} for BC alone to +0.16 W m^{-2} (or by −0.04 W m^{-2}) for a global mean OC burden of approximately 0.7 mg m^{-2}. However, if OC were modeled as an external mixture with BC and/or if the effects of relative humidity are included, the radiative forcing due to OC from fossil fuels is likely to be more negative, and thus −0.04 W m^{-2} represents an approximate lower limit for the strength of the forcing due to fossil fuel OC. *Cooke et al.* [1999] perform calculations for an external mixture assuming OC is partially absorbing with a modeled ω_0 of approximately 0.97 at a wavelength of 0.55 μm and find a radiative forcing of −0.02 W m^{-2} from a global mean burden of 0.34 mg m^{-2}. If OC were modeled as purely scattering or if the effects of relative humidity were considered, the radiative forcing may be significantly stronger. Thus these modeling estimates suggest an approximate lower limit for the normalized radiative forcing for OC of approximately −60 W g^{-1}, which is significantly smaller in magnitude than that due to BC or sulphate aerosol. This may be due to the modeling studies using different size distributions based on observations, which yield lower extinction efficiencies than for sulphate aerosols, and to smaller hygroscopic effects [*Penner et al.*, 1998].

2.3.3. Biomass-burning BC and OC. The annual mean radiative forcing due to biomass-burning aerosol where BC and OC are combined has been studied by *Hobbs et al.* [1997], *Iacobellis et al.* [1999], *Penner et al.* [1998], and *Grant et al.* [1999]. *Hobbs et al.* [1997] performed aircraft measurements of smoke from biomass burning during the Smoke, Clouds, and Radiation–Brazil (SCAR–B) experiment and used the model of *Penner et al.* [1992] to estimate a global mean radiative forcing of −0.3 W m^{-2} as an approximate upper limit for OC and BC combined. *Penner et al.* [1998] and *Grant et al.* [1999] perform 3-D GCM modeling studies of the radiative forcing of OC and BC combined as an internal mixture and determine a radiative forcing of between −0.14 and −0.21 W m^{-2} depending upon the assumed optical parameters. *Iacobellis et al.* [1999] calculate the radiative forcing due to biomass-burning BC and OC combined to be −0.7 W m^{-2} but use an emission factor that *Liousse et al.* [1996] suggest may be a factor of 3 too high, leading to a possible overestimate of the atmospheric burden. Additionally, the specific extinction coefficient used by *Iacobellis et al.* [1999] is significantly larger than those of *Penner et al.* [1998], who base their model calculations upon observed extinction coefficients; thus *Iacobellis et al.* [1999] calculate a larger normalized radiative forcing (see Table 3).

2.3.4. Other studies. The radiative forcing for BC from both fossil fuels and biomass burning has been studied by *Haywood and Ramaswamy* [1998] and *Hansen et al.* [1998]. *Haywood and Ramaswamy* [1998] determine a radiative forcing due to combined biomass and fossil fuel sources of +0.4 W m^{-2}; approximately half of this radiative forcing is attributed to fossil fuel and half is

attributed to biomass burning. *Hansen et al.* [1998] used a different approach and adjusted the single scattering albedo of purely scattering sulphate and organic aerosols from unity to 0.92–0.95 to account for the absorption characteristics of BC. *Hansen et al.* [1998] used the geographical distribution of OC derived from the chemical transport model of *Liousse et al.* [1996] to estimate the radiative forcing due to purely scattering fossil fuel and biomass OC to be -0.41 W m^{-2}.

The geographic distribution of the radiative forcing of fossil fuel BC and OC combined from the study of *Penner et al.* [1998] is shown in Plate 1b. Because the contribution to the global mean radiative forcing due to fossil fuel OC is relatively small (see Table 3), the radiative forcing tends to be positive almost everywhere due to the strong absorption characteristics of BC (see section 2.1 and Figures 2 and 3). The geographic distribution of the radiative forcing of biomass-burning BC and OC combined from the study of *Penner et al.* [1998] is shown in Plate 1c. The radiative forcing is calculated to be negative over the majority of the globe, but some limited areas of positive forcing exist over areas with a high surface reflectance, due to the dependence of the radiative forcing upon the underlying surface albedo (see section 2.1 and Figures 2 and 3) and the partially absorbing nature of combined OC and BC.

2.4. Mineral Dust Aerosol

Mineral dust is created by wind erosion of arid areas of the Earth. Dust production is typically parameterized in transport models as a function of the vegetation fraction and surface wind speed and includes a soil moisture–dependent threshold velocity below which no dust is produced. Recent studies have suggested that between 20% and 50% of the total mineral dust in the atmosphere originates from anthropogenic activities [*Sokolik and Toon*, 1996; *Tegen and Fung*, 1995]. Determination of the anthropogenic fraction of mineral dust in the atmosphere is exceedingly difficult for many reasons. There is no physically based inventory of emissions except from models. Additionally, the influence of anthropogenic activity upon land-use change is difficult to determine because it is likely that some changes occur due to natural climate variability or as a feedback in response to changing atmospheric conditions [e.g., *Myhre and Stordal*, 2000]. Here only the radiative forcing from this anthropogenic component is considered, as there is no evidence that the naturally occurring component has changed since 1750. However, over longer timescales, ice core measurements suggest that atmospheric concentrations of dust have varied substantially, with significantly more mineral dust deposited in the Antarctic and Greenland ice sheets during the Last Glacial Maximum [e.g., *Reader et al.*, 1999, and references therein]. Because mineral dust particles are of a large size and because they become lofted to high altitudes in the troposphere, in addition to the solar radiative forcing, dust may exert a significant thermal infrared radiative forcing. The global mean radiative forcing will be negative in the solar part of the spectrum, due to the predominantly scattering nature of mineral dust aerosol at these wavelengths, and positive in the thermal infrared.

Sokolik and Toon [1996] estimated the anthropogenic contribution to the dust loading due to changes in land use associated with anthropogenic activity to be 20% of the total dust burden and neglected forcing in cloudy regions to estimate a solar radiative forcing of -0.25 W m^{-2} over ocean and -0.6 W m^{-2} over land, leading to a global forcing of approximately -0.46 W m^{-2}. They point out that this is offset to some extent by a positive thermal infrared forcing. *Tegen and Fung* [1995] modeled dust aerosol and estimated that approximately 30–50% of the total dust burden is due to changes in land use associated with anthropogenic activity. The radiative forcing using these data was estimated by *Tegen et al.* [1996] to be -0.25 W m^{-2} in the solar spectrum and $+0.35$ W m^{-2} in the thermal infrared, resulting in a net radiative forcing of $+0.09$ W m^{-2}. Updated calculations of the net radiative forcing based on the work of *Miller and Tegen* [1998] estimate the radiative forcing to be -0.22 W m^{-2} in the solar spectrum and $+0.16$ W m^{-2} in the thermal infrared, resulting in a net radiative forcing of -0.06 W m^{-2}. *Hansen et al.* [1998] perform similar calculations and calculate a net radiative forcing of -0.12 W m^{-2} by assuming a different vertical distribution and different optical parameters and using a different global model. These global studies have considered mineral dust as a homogeneous mixture of minerals; that is, they have used a constant refractive index that is independent of the mineral composition of the aerosols. More recent studies have started to incorporate the mineral composition as a function of the dust sources [e.g., *Claquin et al.*, 1999; *Sokolik and Toon*, 1999] and have examined the effect of the optical parameters. *Myhre and Stordal* [2000] perform a sensitivity study of the effects of mineral dust using a global model and two different 3-D data sets for mineral dust. They investigate the effects of altitude, size distribution, and refractive index and find a large sensitivity in the radiative forcing to each, but particularly to the assumed refractive index, which is dependent upon the mineral composition. The effects of nonsphericity of the mineral dust are not accounted for in any of these calculations. *Mishchenko et al.* [1997] model dust particles as spheroids and suggest that differences in the optical parameters between model spheroids and spheres do not exceed 10–15%, although changes of this magnitude may have a large effect on the radiative forcing [*Miller and Tegen*, 1998]. An example of the geographical distribution of the radiative forcing is shown in Plate 1d [*Tegen et al.*, 1996]. This shows regions of positive and negative forcing. Positive forcing tends to exist over regions of high surface reflectance, and negative radiative forcings tend to exist over areas of low surface reflectance due to the dependence of the forcing on surface reflectance, as

described in section 2.1, and the additional effects of the longwave radiative forcing.

One problem that needs to be solved is uncertainty in representative refractive indices [*Claquin et al.*, 1998]. The modeling study of *Hansen et al.* [1998] calculates that the net radiative forcing changes from -0.12 to -0.53 W m^{-2} when dust is treated as conservatively scattering. *Sokolik et al.* [1993] present a summary of solar imaginary refractive indices from many geographical locations showing a range of $-0.003i$ to $-0.009i$ at 0.55 μm. Differences in refractive index in the thermal infrared from different geographical sources are also reported by *Sokolik et al.* [1998]. *von Hoyningen-Huene et al.* [1999] determine the imaginary part of the refractive index from surface-based absorption and scattering measurements and find that a refractive index of $-0.005i$ best fits the observations. The radiative forcing is particularly sensitive to the single scattering albedo [*Miller and Tegen*, 1999]. Additional uncertainties lie in modeling the size distributions [*Tegen and Lacis*, 1996; *Claquin et al.*, 1998] that together with the refractive indices, determine the optical parameters. Although there have been a growing number of estimates of the local, clear-sky radiative effect and optical depths of Saharan dust from satellite instruments [e.g., *Ackerman and Chung*, 1992; *Swap et al.*, 1996; *Goloub et al.*, 1999], relating instantaneous observational measurements that do not account for the effects of clouds, diurnal averaging of the radiation, the seasonal signal associated with emissions, and the fraction of mineral dust that is anthropogenic to the global mean radiative forcing is very difficult. Note also that the effects of stratospheric adjustment have not been considered in any study to date: This is likely to be more important for tropospheric aerosols that are lofted to high altitudes in the troposphere, such as mineral dust. Because the resultant global mean net radiative forcing is a residual obtained by summing the solar and the thermal infrared radiative forcings that are of roughly comparable magnitudes, the uncertainty in the radiative forcing is large, and even the sign is in doubt due to the competing nature of the solar and thermal infrared effects.

2.5. Nitrate Aerosol

Although *IPCC* [1994] identified nitrate aerosol as a significant anthropogenic source of aerosol, there have been few studies of the direct radiative effect. *Adams et al.* [1999] perform a global chemical modeling study of sulfate, nitrate, and ammonium aerosol and estimate a global mean burden of approximately 0.13 Tg NO_3 (0.25 mg m^{-2}). Also, *van Dorland et al.* [1997] have produced a radiative forcing estimate of approximately -0.03 W m^{-2} for ammonium nitrate, but as acknowledged by the authors, many of the assumptions implicit within the calculations make this a first-order estimate only. Recent measurement studies by *Veefkind et al.* [1996] and *ten Brink et al.* [1997] in the Netherlands have shown that nitrate aerosol in the form of ammonium nitrate is a locally important aerosol species in terms of aerosol mass in the optically active submicron size range and hence in the associated local radiative forcing. They also emphasize the problems in measuring the concentrations and size distributions of nitrate, which is a semivolatile substance. The paucity of global studies of this aerosol species means that an assessment of the radiative forcing due to anthropogenic nitrate aerosol is not possible at the present time.

2.6. Mixed Aerosols

Most of the global modeling studies performed to date consider tropospheric aerosol to be externally mixed (i.e., each aerosol chemical species exists independently of the others), which makes modeling the sources, atmospheric transport, and radiative properties simpler [e.g., *Tegen et al.*, 1997; *Haywood et al.*, 1999]. However, single particle analysis of particles containing mineral dust [e.g., *Levin et al.*, 1996] and sea salt [e.g., *Murphy et al.*, 1998] have often shown them to be internally mixed with sulphate and other aerosols of anthropogenic origin. This means that submicron particles such as anthropogenic sulphate may be removed from the optically active region through heterogeneous processes and become internally mixed with larger supermicron species [e.g., *Dentener et al.*, 1996], an effect that has not yet been accounted for in global modeling studies. Global studies that examine the radiative forcing of absorbing and scattering particles such as BC and sulphate [e.g., *Haywood et al.*, 1997a; *Myhre et al.*, 1998; *Chýlek et al.*, 1995] suggest that an internal mixture may be more absorbing than a corresponding external mixture. Also, *West et al.* [1998] suggest that for internally mixed aerosol particles containing sulphate, the radiative forcing may not increase monotonically with sulphate loading due to chemical interactions between sulphate and other chemical components such as ammonium, nitrate, and water. Additionally, *McInnes et al.* [1998] suggest that OC may act to suppress the hygroscopic nature of sea salt and sulphate; thus the effect of OC emissions may, under certain circumstances, result in a net positive forcing. Thus it is very unlikely that the radiative forcing from different species will add linearly. Further modeling work where all aerosol types, including natural species, are included in chemical transport models is necessary if the effects of internal mixing upon the overall radiative forcing are to be assessed on a global scale.

2.7. Field Campaigns

Field campaigns such as the Tropospheric Aerosol Radiative Forcing Observational Experiment (TARFOX) and the Aerosol Characterization Experiment (ACE 1 and 2), the Indian Ocean Experiment (INDOEX) and SCAR–B (Smoke, Clouds, and Radiation–Brazil), and long-term monitoring networks such as Aerosol Robotic Network (AERONET) provide essential information on the chemical, physical, and optical properties of aerosol particles, without which it would be impossible to vali-

date assumptions used in modeling studies [e.g., *Novakov et al.*, 1997; *Hegg et al.*, 1997; *Murphy et al.*, 1998; *Hobbs et al.*, 1997; *Ross et al.*, 1998; *Holben et al.*, 1998]. TARFOX has helped validate current treatment of radiative transfer by comparing in situ radiances and irradiances with those predicted by radiation codes using in situ observations of aerosol chemical composition and morphology and atmospheric concentrations. *Hignett et al.* [1999] modeled TARFOX aerosol as an internal mixture of sulphate, OC, and BC and used in situ aircraft observations to show the importance of the BC component in obtaining good agreement between modeled and observed broadband irradiances. Similar calculations were performed by *Russell et al.* [1999], who also showed good agreement between modeled and measured irradiances and that the strongest forcing occurred not at midday but when the solar zenith angle was approximately 60°–70°, in agreement with theoretical calculations (see Figure 4). *Francis et al.* [1999] made similar modeling assumptions and found reasonable agreement between the modeled and measured radiances, indicating that the scattering phase function was in reasonable agreement with theory. The hygroscopic growth factor of the aerosol was investigated in detail by *Kotchenruther et al.* [1999], who found different growth factors for different large-scale flow regimes and that, on average, the direct radiative forcing at 80% relative humidity was approximately double that of the dry aerosol. The results from TARFOX suggest that under certain circumstances, the use of an internal mixture may be more appropriate for modeling the physical and radiative properties of aerosols (see section 2.6) rather than the assumption of external mixtures that have been widely used in modeling studies. INDOEX provided information on the chemical, physical, and optical properties of aerosols in the Indian Ocean, chemical analysis revealing that aerosol can be transported for thousands of kilometers from the source regions [*Podgorny et al.*, 2000; *Satheesh et al.*, 1999]. A significant degree of absorption due to the large quantities of atmospheric BC aerosol was noted, as evidenced by the fact that the change in irradiance at the surface was 2–3 times that observed at the top of the atmosphere [*Podgorny et al.*, 2000]. This means that there is a vertical redistribution of energy throughout the atmosphere that does not occur with purely scattering aerosols. Modeling studies suggest that for absorbing aerosols, the climate sensitivity parameter λ may differ significantly due to diabatic heating in the aerosol layer modifying the temperature structure of the atmosphere, which may affect the formation of clouds [*Hansen et al.*, 1997b]. SCAR–B studied biomass-burning aerosol over Brazil and provided important information on the refractive indices [e.g., *Yamasoe et al.*, 1998], size parameters [e.g., *Remer et al.*, 1998], optical parameters [e.g., *Dubovik et al.*, 1998], relative humidity growth factors [e.g., *Ross et al.*, 1998], and radiative effects [e.g., *Eck et al.*, 1998; *Ross et al.*, 1998] of biomass-burning aerosol. *Hobbs et al.* [1997] highlight the significant absorption of biomass-burning aerosols and the fact that biomass-burning aerosol is not as hygroscopic as industrial aerosol measured off the coast of the continental United States (see also *Kotchenruther et al.* [1999] and *Ross et al.* [1998]). ACE 2 provided much information on the physical characteristics of aerosol over the eastern Atlantic. *Russell and Heintzenberg* [2000] summarize a variety of column closure experiments for Saharan dust and for marine boundary-layer aerosol performed during the campaign and highlight differences between observed and calculated aerosol optical depths due to particle shapes, complex refractive indices, and single scattering albedos. *Schmid et al.* [2000] perform local closure experiments for aerosol size distributions and aerosol optical depths using in situ measurements of the size distributions and Sun-photometer data and find excellent agreement despite the fact that the desert dust aerosols are assumed to be spherical. *Haywood et al.* [2000] use aircraft measurements of the scattered radiance at 0.55 μm in a Saharan dust layer and find good agreement with modeling calculations that assume spherical particles. These studies suggest that for reasonable accuracy in radiative calculations, dust particles may be modeled as spheres (see section 2.4). Field campaigns have helped verify our understanding of radiative transfer and aerosol physical properties and thus are extremely valuable in verifying assumptions for input parameters in global modeling studies. However, note that the limited-area nature of measurement campaigns and the difficulties in distinguishing between aerosols from anthropogenic and natural sources mean that global models remain necessary in estimating the global radiative forcing.

2.8. Satellite Measurements

Remote sensing of aerosols has made considerable progress in the past few years [*King et al.*, 1999]. Spaceborne instruments, such as the advanced very high resolution radar (AVHRR) [*Husar et al.*, 1997; *Nakajima and Higurashi*, 1998; *Higurashi and Nakajima*, 1999] and Meteosat [e.g., *Jankowiak and Tanré*, 1992; *Moulin et al.*, 1997], have proven useful in retrieving aerosol optical depth. More recently dedicated instruments, such as Polarization and Directionality of the Earth's Reflectance (POLDER) [*Goloub et al.*, 1999; *Deuzé et al.*, 1999], Moderate-Resolution Imaging Spectroradiometer (MODIS) [*King et al.*, 1992; *Kaufman et al.*, 1997; *Tanré et al.*, 1997], Ocean Color Temperature Scanner (OCTS) [*Nakajima et al.*, 1999], or Along Track Scanning Radiometer (ATSR) [*Veefkind et al.*, 1999], have been designed to monitor aerosol properties, and accurate retrieval of the aerosol optical depth over the ocean in clear-sky conditions has proved to be feasible [*Goloub et al.*, 1999; *Tanré et al.*, 1999; *Veefkind et al.*, 1999].

Cusack et al. [1998] report better agreement between GCM clear-sky top and bottom of atmosphere irradiances over oceans and observations from Earth Radiation Budget Experiment (ERBE) and Scanner for Ra-

diation Budget (ScaRab) when a simple aerosol climatology is included. *Haywood et al.* [1999] find that inclusion of chemical transport model based aerosol climatologies and radiative effects can explain much of the magnitude and the spatial distribution of differences between GCM modeled and observed ERBE irradiances over oceans. Plate 2 shows an example of the radiative effect of tropospheric aerosols as computed from the POLDER aerosol retrievals [*Boucher and Tanré*, 2000]. The radiative signatures of biomass-burning aerosols and the Saharan dust plume off the coast of west Africa and that of industrial aerosols off the east coast of the United States and over the Mediterranean Sea are clearly visible. There is also a clear seasonal variation in the aerosol radiative effects.

Aerosol retrievals over land are also developing rapidly but are complicated by the spectral and angular dependence of the surface reflectivity [e.g., *Leroy et al.*, 1997; *Wanner et al.*, 1997]. *Soufflet et al.* [1997] developed an aerosol retrieval algorithm over dark land surfaces using AVHRR. *Kaufman et al.* [1997] undertake a similar approach with the MODIS instrument. *M. Herman et al.* [1997] suggest that the surface contribution could be more easily corrected for the polarized radiances than for the total radiances, which would allow the retrieval of the aerosol optical depth over land. *Flowerdew and Haigh* [1996] and *Veefkind et al.* [1998] used the dual-look capability of the ATSR 2 instrument in order to retrieve the aerosol optical depth over land by assuming that the ratio of the surface reflectances in the two viewing directions is independent of the wavelength. *Li and Kou* [1998] determine the radiative effect of smoke over visible wavelengths using GOES data over boreal forests in western Canada, where the surface reflectance is also relatively invariant. The infrared radiances from Meteosat (and other sensors) can also be used to detect desert dust events over bright surfaces [*Legrand et al.*, 1989; *Ackerman*, 1997] and diagnose their radiative impact. The Total Ozone Mapping Spectrometer (TOMS) instrument [*J. Herman et al.*, 1997] has the capability to detect partially absorbing aerosols over land and ocean, but the measured signal is a function of the vertical distribution of aerosols and therefore remains semi-quantitative.

In addition to aerosol optical depth, the Angström coefficient can also be retrieved with reasonable agreement when compared with ground-based Sun-photometer data [*Goloub et al.*, 1999; *Nakajima and Higurashi*, 1998; *Higurashi and Nakajima*, 1999]. The Angström coefficient gives an indication of the vertically averaged size distribution of the aerosol particles. The retrieval of the single scattering albedo, which is important in predicting the sign of the direct radiative forcing, is still an unresolved issue despite exploratory studies [*Kaufman*, 1987]. Although satellite measurements of aerosols will undoubtedly help in estimating the aerosol direct radiative forcing and validating model predictions of the global aerosol cycles in the future, there are few studies on this topic to date. Moreover, the problem of separating the natural from the anthropogenic components of the atmospheric aerosols remains, although the Angström coefficient can discriminate between primary and secondary aerosols [*Boucher and Tanré*, 2000]. In particular, the fraction of emitted dust that originates from changes in land use remains very uncertain. Finally, aerosol retrieval is usually associated with a stringent cloud-screening algorithm, which raises the issue of the representativeness of sampled (cloud-free) pixels. In particular, aerosol retrievals over and close to cloudy regions are not possible. In this perspective, future satellite lidar measurements are very promising. Despite these potential problems, it is very likely that more and more global modeling efforts will use satellite retrievals of the clear-sky radiative effect or the optical depth to help better constrain the radiative effects of aerosols, particularly when the models incorporate all of the natural and anthropogenic aerosol components discussed here.

2.9. Discussion of Uncertainties of Direct Effect

While the radiative forcing due to greenhouse gases may be determined to a reasonably high degree of accuracy [*IPCC*, 1996], the range of estimates due to aerosol direct radiative forcings remains large, and estimations of the aerosol forcing rely to a large extent on global modeling studies that are difficult to verify at the present time. The range of estimates presented in this section represents the structural uncertainties (i.e., differences in the model structures and assumptions) rather than the parametric uncertainties (i.e., the uncertainties in the key parameters such as optical parameters, burden, and so on [see *Pan et al.*, 1997]). Three major areas of uncertainty exist: uncertainties in the atmospheric burden, uncertainties in the optical parameters, and uncertainties in implementation of the optical parameters and burden to give a radiative forcing. The atmospheric burden of an anthropogenic aerosol species is determined by factors such as combustion, emission, aging, convective transport, and scavenging processes, each of which has an associated uncertainty. The optical parameters have associated uncertainties in size distribution, chemical composition, state of mixing, method of mixing, and asphericity. Uncertainties in calculating the radiative forcing from specified burdens and optical parameters arise from uncertainties in the parameterization of relative humidity effects; the horizontal and vertical distributions of the aerosol; the uncertainties and subgrid-scale effects in other model fields such as clouds, humidity, temperature, and surface reflectance; the representation of the diurnal cycle; and the accuracy of the radiation code used in the calculations. Accurate satellite retrievals of aerosol radiative effects show promise for helping to constrain estimates of the model input parameters such as size distribution as well as to constrain the radiative effects on a close to global scale. While the general spatial distribution of the radiative

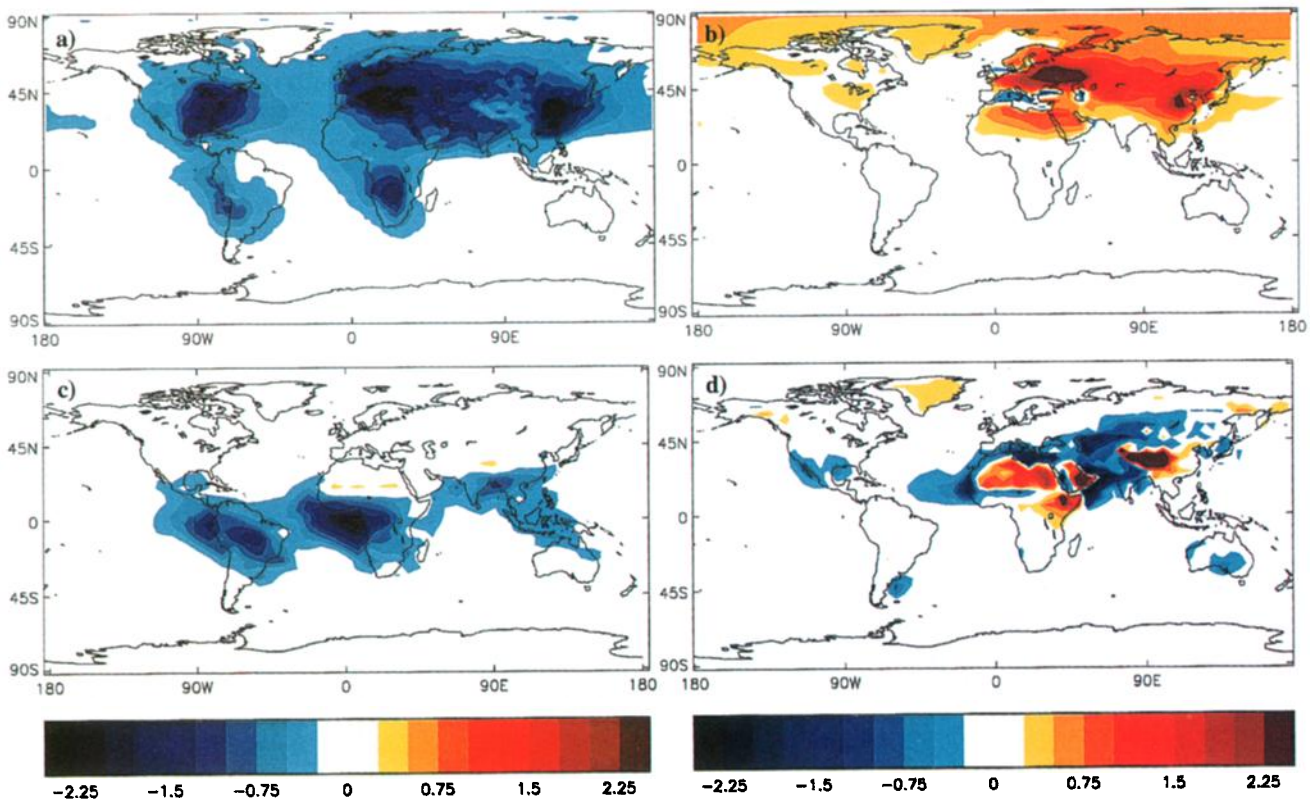

Plate 1. Examples of the radiative forcing (W m^{-2}) due to (a) the direct effect of sulphate aerosol [*Haywood et al.*, 1997a], (b) the direct effect of organic carbon and black carbon from fossil fuel burning [*Penner et al.*, 1998; *Grant et al.*, 1999], (c) the direct effect of organic carbon and black carbon from biomass burning [*Penner et al.*, 1998; *Grant et al.*, 1999], and (d) the direct effect of anthropogenic emissions of mineral dust [*Tegen et al.*, 1996]. Different modeling studies may show substantially different spatial patterns, as described in the text.

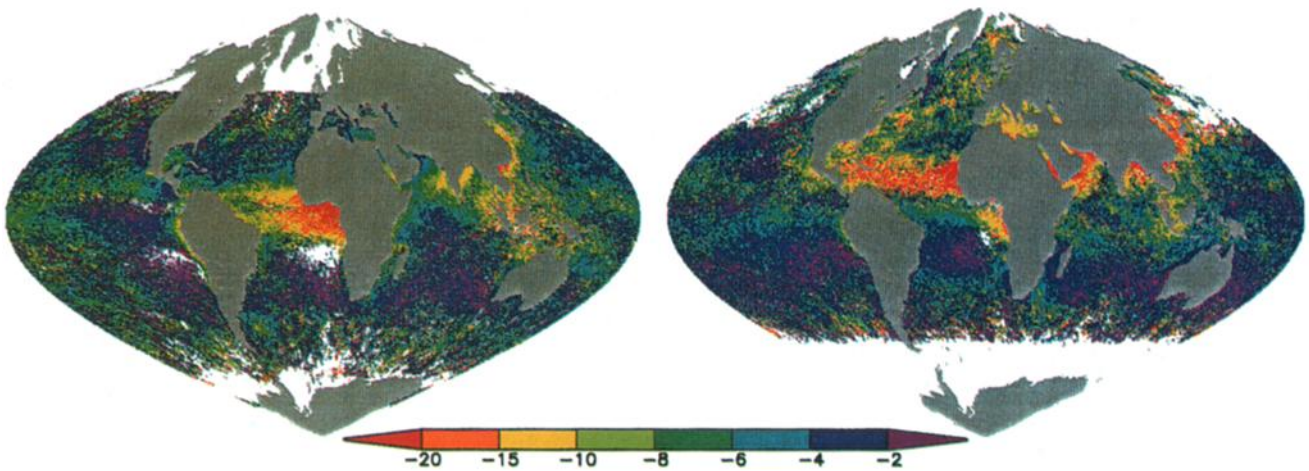

Plate 2. Clear-sky shortwave radiative perturbation (W m^{-2}) computed from POLDER aerosol retrieval for (left) December 1996 and (right) June 1997 [from *Boucher and Tanré*, 2000].

forcing for sulphate aerosol from different studies appears to be similar, some important features such as the seasonal cycle in the radiative forcing remain highly uncertain, which may have important consequences in terms of the detection and attribution of climate change. Additionally, we have concentrated specifically upon the radiative forcing of anthropogenic aerosol species; a further uncertainty highlighted by *Hansen et al.* [1997b] is that for absorbing aerosols, the climate sensitivity parameter λ may differ significantly due predominantly to the feedback effect of clouds.

3. INDIRECT RADIATIVE FORCING

Aerosols serve as cloud condensation and ice nuclei. An increase in aerosol concentration and/or properties can therefore modify the microphysical and radiative properties of clouds, as well as the precipitation efficiency and hence the cloud lifetime. A review of theoretical and observational evidence for the aerosol indirect effects is given by *Schwartz and Slingo* [1995]. The observational evidence includes measurements of an anthropogenic influence on cloud condensation nuclei (CCN) concentrations [e.g., *Hegg et al.*, 1993], correlative measurements of sulphate or aerosol concentrations and cloud droplet number concentration [e.g., *Leaitch et al.*, 1992; *Martin et al.*, 1994; *Novakov et al.*, 1994], and studies of the so-called "ship track" phenomenon [e.g., *Coakley et al.*, 1987; *Radke et al.*, 1989]. Recently, the ACE 2 CloudyColumn experiment focused on the contribution of stratocumulus clouds to the indirect effect in June–July between Portugal and the Canary Islands [*Brenguier et al.*, 2000a]. Significantly larger cloud droplet number concentrations and smaller cloud droplet size were reported for clouds formed in air masses of continental origin compared with air masses of marine origin [*Brenguier et al.*, 2000b]. A clear comparison of the cloud visible reflectance or cloud optical depth between polluted and nonpolluted clouds is complicated by the fact that these clouds have different geometrical thicknesses. When the effect of geometrical thickness is accounted for, a correlation is found between the cloud optical depth and the cloud droplet number concentration, albeit with considerable scatter [*Brenguier et al.*, 2000b, Figure 6b]. It should be noted that there are, to date, no convincing observations showing the entire chain of processes of the aerosol indirect effect from enhanced aerosol concentrations to enhanced cloud albedo on a scale large enough to influence significantly the Earth's radiation budget. This is due, in particular, to the large variability in the cloud albedo parameter due to the large natural variability in cloud types and cloud liquid water path.

Below, we review and discuss the various estimates of the globally averaged aerosol indirect radiative forcing by anthropogenic aerosols. Because of the inherent complexity of the aerosol indirect effect, GCM studies dealing with its quantification necessarily include a significant degree of simplification. While this is a legitimate approach, it should be clear that GCM estimates of the aerosol indirect effect are very uncertain. Section 3.1 investigates the indirect radiative forcing due to sulphate aerosols, on which most efforts have concentrated, while other aerosol types are treated in section 3.2. Section 3.3 is devoted to alternative approaches, while section 3.4 investigates the aerosol indirect effects on ice clouds.

3.1. Sulphate Aerosols

3.1.1. Estimates of the cloud albedo effect. The indirect radiative forcing by sulphate aerosols has received a lot of attention since *IPCC* [1996]. Table 4 reports the studies available in the literature. These studies use different GCMs and different methods for computing the droplet number concentration. While some authors [e.g., *Boucher and Lohmann*, 1995] used empirical relationships between the sulphate mass and the cloud droplet number concentration, other studies [e.g., *Jones et al.*, 1994] rely on empirical relationships between the sulphate aerosol number concentration and the cloud droplet number concentration. In the latter case one has to assume a size distribution for sulphate aerosols to convert the sulphate mass concentration predicted by the CTM or GCM into an aerosol number concentration. Among the most recent studies, *Chuang et al.* [1997], *Lohmann et al.* [2000], and *Ghan et al.* [2000a] developed parameterizations of the cloud nucleation process. This approach (sometimes referred to as a "mechanistic" approach) accounts for other preexisting aerosol types and variations in the cloud vertical updraft and avoids the problem of prescribing a unique relationship between aerosol mass and cloud droplet concentration. While this represents a more comprehensive approach, it also adds to models one degree of complexity by introducing a process not yet fully understood. Some of the relationships are plotted in Figure 5. A comparison between diagnostic and prognostic relationships is not straightforward. For *Jones et al.* [1999], over the ocean the relationship also depends on the sea-salt concentration. The best fit between sulphate mass and cloud droplet number concentration obtained with the *Lohmann et al.* [2000] parameterization is also due to other aerosol types, which are correlated to sulphate aerosols and also serve as cloud condensation nuclei. Figure 5 nevertheless suggests that the empirical relationships used by the first investigators show the same qualitative behavior as the new "mechanistic" parameterizations, although, of course, they cannot be considered as universally valid.

One can see from Table 4 that the radiative forcing estimates for the cloud albedo effect range from -0.3 to -1.8 W m^{-2}, which is close to the range of 0 to -1.5 W m^{-2} given by *IPCC* [1996] when only a few estimates were available. There does not seem to be an obvious relationship between the level of model complexity and

TABLE 4. The Global-Mean Annual-Average Indirect Radiative Forcing Due to Aerosols From Different Global Studies

Reference	Aerosol Type	Forcing Estimate, W m^{-2}			Remarks
		Cloud Albedo	Cloud Lifetime	Both Effects	
Boucher and Rodhe [1994][a]	SO_4			−0.65 to −1.35	(P) use three relationships between SO_4 mass and CCN/CDN concentrations
Chuang et al. [1994]	SO_4	−0.47			(C) include a parameterization of cloud nucleation processes
Jones et al. [1994]	SO_4	−1.3			(P) use a relationship between aerosol and droplet number concentrations
Boucher and Lohmann [1995]	SO_4	−0.5 to −1.4 −0.45 to −1.5			(P) LMD, GCM } use four different relationships between SO_4 mass (P) ECHAM } and CCN/CDN concentrations (A, B, C, and D)
Jones and Slingo [1996]	SO_4	−0.3 to −1.5			(P) use two different SO_4 distributions; follow *Jones et al.* [1994] and *Boucher and Lohmann* [1995] "D"
Kogan et al. [1996, 1997]	SO_4	−1.1			use a cloud climatology rather than GCM-simulated clouds
Chuang et al. [1997]	SO_4	−0.4 to −1.6			(C) include a parameterization of cloud nucleation processes; use a mixture of preexisting aerosols
Feichter et al. [1997]	SO_4	−0.76			(C) use *Boucher and Lohmann* [1995] "A" relationship
Jones and Slingo [1997]	SO_4	−0.55 to −1.50			(P) use two different versions of the Hadley Centre model
Lohmann and Feichter [1997][a]	SO_4	−1		−1.4 to −4.8	(C) use *Boucher and Lohmann* [1995] "A" relationship
Rotstayn [1999][a]	SO_4	−1.1 to −1.7	−0.4 to −1.0	−1.6 to −3.2	(P) include a (small) LW radiative forcing
Jones et al. [1999][a,b]	SO_4	−0.91	b.e. −0.66	−1.18	(C) include a (small) LW radiative forcing; the two effects add nonlinearly
Kiehl et al. [2000]	SO_4	−0.40 to −1.78			(C)
Lohmann et al. [2000][a]	SO_4			0 to −0.4	(C)
	carb			−0.9 to −1.3	(C) include a parameterization of cloud nucleation
	both	~40%	~60%	−1.1 to −1.5	(C)
Ghan et al. [2000a][a]	SO_4	~50%	~50%	−1.6 to −3.2 (b.e. −1.7)	(C) include a parameterization of cloud nucleation; predicted aerosol size distribution

Letters P (prescribed) and C (computed) refer to off-line and on-line SO_4 aerosol calculations, respectively; CCN and CDN stand for cloud condensation nuclei and cloud droplet number, respectively; "b.e." stands for best estimate; "carb" stands for carbonaceous aerosols.

[a]The estimate in flux change due to the indirect effect of aerosols was computed as the difference in top-of-atmosphere fluxes between two distinct simulations and therefore does not represent a forcing in the strict sense.

[b]Predicts SO_4 concentrations which are too small on average.

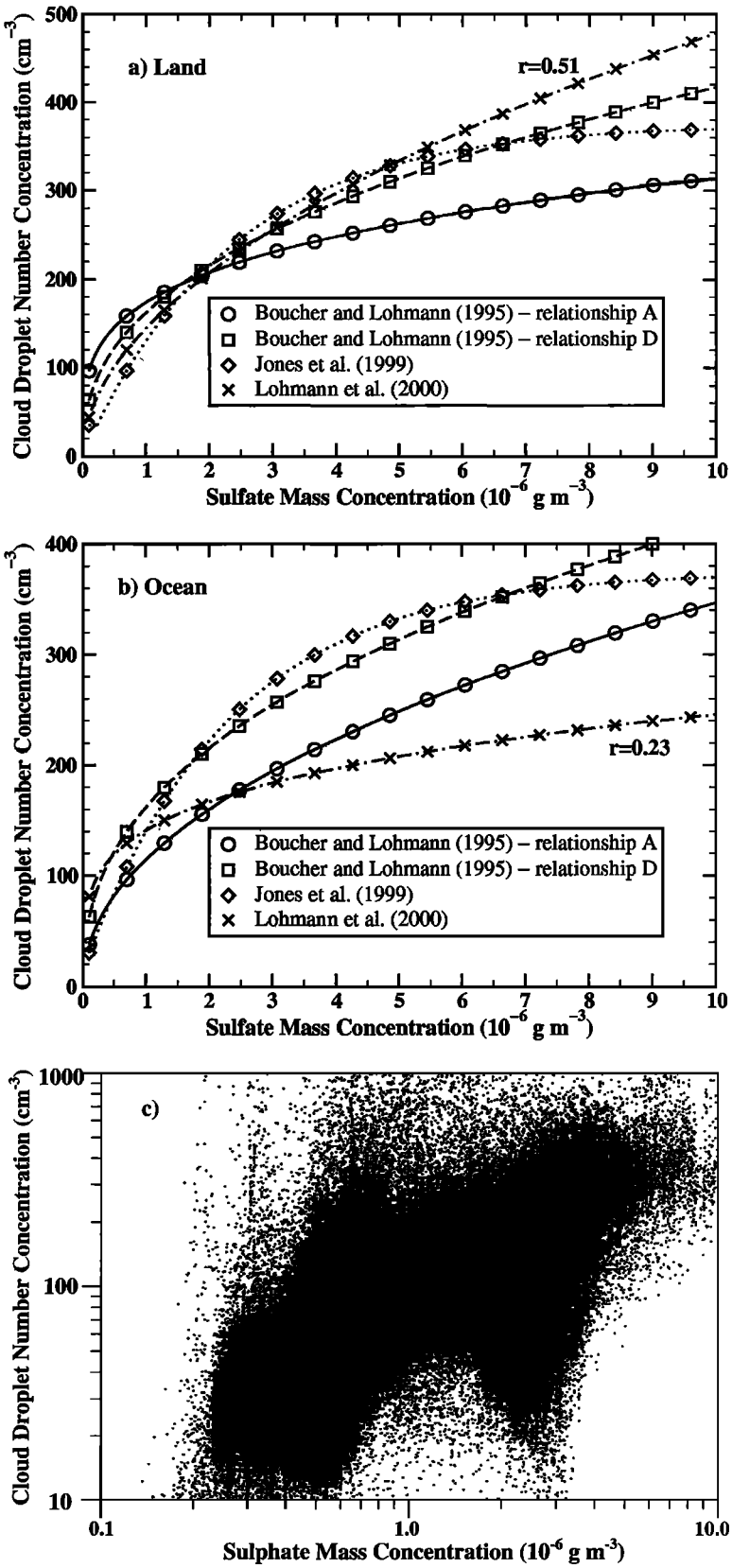

Figure 5. Cloud droplet number concentration as a function of sulphate mass concentration over (a) land and (b) ocean. The empirical relationships of *Boucher and Lohmann* [1995] and *Jones et al.* [1999] are shown, along with a best fit obtained with the mechanistic parameterization of *Lohmann et al.* [2000]. The correlation coefficient is indicated for the *Lohmann et al.* [2000] fit to the data. The relationship obtained by *Ghan et al.* [2000a] is displayed as a separate scatterplot in Figure 5c. See text for more details.

the magnitude of the forcing, as each of the approaches discussed above leads to a rather large range of forcings. There is a tendency for more and more studies to use interactive (on-line) rather than prescribed (monthly- or annual-mean) sulphate concentrations. *Feichter et al.* [1997] pointed out that the first indirect effect calculated from monthly-mean sulphate concentrations is 20% larger than that calculated from interactive sulphate concentrations. *Jones et al.* [1999] found that the total indirect effect was overestimated by about 60% if they used seasonal- or annual-mean sulphate concentrations.

The various GCM studies show some disagreement on the spatial distribution of the forcing, an example of which is shown in Plate 3. The Northern to Southern Hemisphere (NH:SH) ratio varies from 1.4 to 4 depending on the models. It is generally smaller than the NH:SH ratio of anthropogenic sulphate aerosol concentrations because of the higher susceptibility of the clouds in the SH [*Platnick and Twomey*, 1994; *Taylor and McHaffie*, 1994]. The ocean to land ratio depends very much on the type of sulphate mass to cloud droplet number concentration used and on the natural background aerosol concentrations. It was generally found to be smaller than unity [*Boucher and Lohmann*, 1995; *Jones and Slingo*, 1997; *Kiehl et al.*, 2000]. Larger ratios, such as 1.6 [*Chuang et al.*, 1997] and 5 [*Jones and Slingo*, 1997], are reported in some of the GCM sensitivity experiments. Using a detailed inventory of ship sulphur emissions and a simple calculation of the aerosol indirect effect, *Capaldo et al.* [1999] suggested that a significant fraction of the effect over the oceans (-0.11 W m^{-2}, averaged globally) could be due to ship-emitted particulate matter (sulphate plus organic material in this case). So far, this source of aerosols has not been included in the GCM studies.

Kogan et al. [1996, 1997] used the *Warren et al.* [1988] cloud climatology over the oceans rather than a GCM to predict the indirect effect by sulphate aerosols on cloud albedo. The cloud albedo susceptibility was evaluated from a large eddy simulation model applied to stratocumulus clouds. They found an indirect shortwave forcing of -1.1 W m^{-2} over the oceans, with a small hemispheric difference of 0.4 W m^{-2} (i.e., a NH:SH ratio of about 1.4). In their study the forcing had a strong seasonal cycle, with the SH forcing prevailing in some seasons.

3.1.2. Estimates of the cloud lifetime effect and the combined effects. Whereas the first indirect effect can be computed diagnostically, assessment of the second indirect effect implies that two independent (i.e., with the same fixed sea surface temperatures but with different meteorologies) GCM simulations be made, the first with preindustrial aerosols and the second with present-day aerosols. The difference in top-of-atmosphere fluxes or cloud radiative forcings between two such simulations is used by some authors as a proxy of the forcing due to the second aerosol indirect effect. The simulations need to be sufficiently long (usually 5 years) so that the effects of natural variability can be expected to average out. However, as a consequence, the estimates of the aerosol indirect effect may include some undesirable feedbacks, involving, for instance, changes in the temperature and water vapor fields. There are no studies yet to confirm unambiguously that the radiative impacts associated with the second indirect effect and computed in such a way can be interpreted in the strict sense of a radiative forcing. While some authors call their estimate of the cloud lifetime effect a radiative forcing [e.g., *Rotstayn*, 1999], some others [e.g., *Jones et al.*, 1999] label it as just a radiative effect.

Jones et al. [1999] and *Rotstayn* [1999] provide estimates for the cloud lifetime effect alone with ranges of -0.53 to -2.29 and -0.4 to -1.0 W m^{-2}, respectively. For the combined effect (first and second effects estimated together), *Jones et al.* [1999] and *Rotstayn* [1999] give best estimates of -1.18 and -2.1 W m^{-2}. Larger forcings are found by *Rotstayn* [1999], who uses the parameterization for droplet concentration proposed by *Roelofs et al.* [1998] and *Lohmann and Feichter* [1997], who test two alternative cloud schemes, giving values of -3.2 and -4.8 W m^{-2}, respectively. In contrast, *Lohmann et al.* [2000] predict a much smaller combined effect, with radiative impacts of 0.0 and -0.4 W m^{-2}, assuming externally and internally mixed sulphate aerosols, respectively. The authors attribute this rather small radiative impact to the small increase in anthropogenic sulphate aerosol number concentrations. *Ghan et al.* [2000a] estimate a combined effect of -1.7 W m^{-2} using a mechanistic approach similar to that of *Lohmann et al.* [2000] but with aerosol size distribution predicted rather than prescribed. The larger forcing is due to a variety of differences in the models that remain to be investigated. The studies by *Rotstayn* [1999] and *Jones et al.* [1999] both indicate that the longwave (positive) radiative effect associated with the indirect aerosol effect is small (between 0.0 and 0.1 W m^{-2} for each of the effects).

The partitioning of the total indirect radiative forcing between the first and second effect is uncertain. *Jones et al.* [1999] found that the ratio between their best estimates of the first and second indirect effects, taken separately, was 1.38, while *Lohmann et al.* [2000] predicted a ratio of 0.71 (for sulphate and carbonaceous aerosols taken together). In a set of independent simulations, *Rotstayn* [1999] estimated with his GCM that the radiative impact of the two effects considered together was similar or slightly larger than the sum of the two effects considered separately, depending on the versions of the model being used. In contrast, *Jones et al.* [1999] found that the combined radiative impact (-1.18 W m^{-2}) was less than the sum of the two effects computed separately (estimated as -0.91 and -0.66 W m^{-2}, respectively, corresponding to a total of -1.57 W m^{-2}). This nonadditivity of the radiative impacts implies that some sort of interactions between the two effects are occurring, at least in the model of Jones et al. This suggests that the change in top-of-atmosphere fluxes

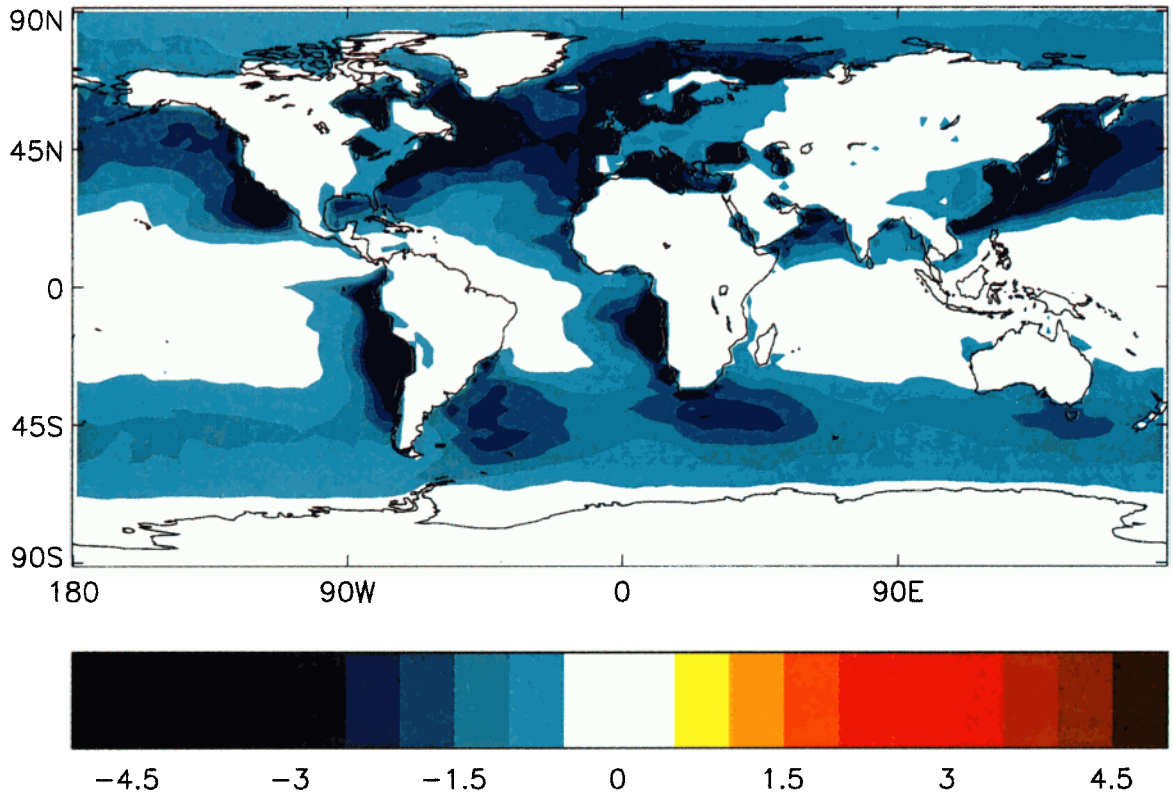

Plate 3. Example of the radiative forcing (W m^{-2}) due to the "first" indirect effect of sulphate aerosol [*Jones and Slingo*, 1997].

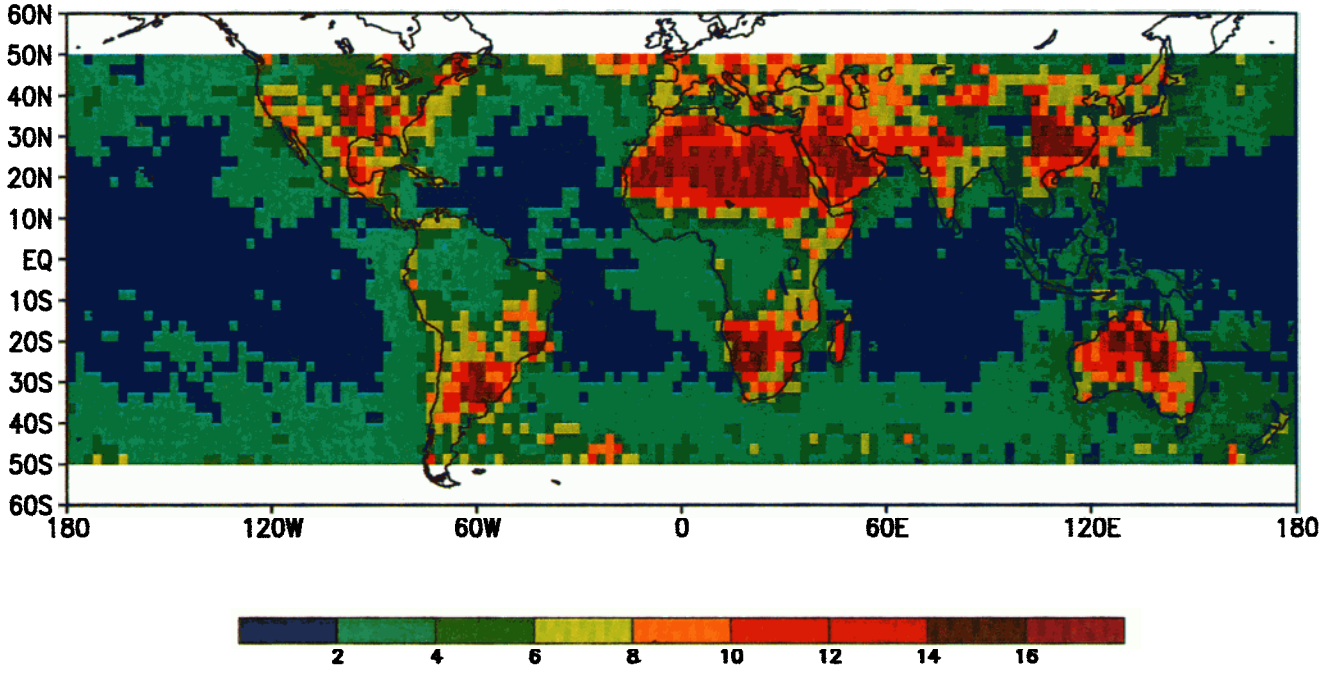

Plate 4. Annual mean cloud column droplet concentration (10^6 cm^{-2}) retrieved from advanced very high resolution radiometer data. Adapted from *Han et al.* [1998b].

between two independent simulations with and without the effects of anthropogenic aerosols constitutes an imperfect quantity in representing the aerosol indirect effect. However, it is recognized that the impact of the second indirect aerosol effect could be a major factor of climate change.

3.1.3. Model evaluation. To date, there is no method for a direct validation of GCM estimates of the aerosol indirect forcing against observations. Nevertheless, global satellite retrievals of various cloud parameters provide indirect means for evaluating and validating the GCM predictions. The simulated cloud droplet effective radii [*Jones et al.*, 1994; *Boucher and Lohmann*, 1995; *Jones and Slingo*, 1996; *Chuang et al.*, 1997; *Jones and Slingo*, 1997; *Roelofs et al.*, 1998; *Rotstayn*, 1999; *Kiehl et al.*, 2000; *Ghan et al.*, 2000b] have been compared with those retrieved from satellite data [*Han et al.*, 1994]. The observed hemispheric and land/ocean contrasts in cloud droplet size are generally simulated by the models, at least qualitatively, the detailed comparison being more or less conclusive depending on the models. It would certainly be appropriate to validate also the horizontal and vertical distribution of the cloud droplet number concentration. This is not yet possible because a global-scale climatology of this parameter does not exist. However, *Han et al.* [1998b] produced a climatology of the column cloud droplet concentration from AVHRR data (Plate 4), which may prove very helpful for model validation. General circulation models with a predictive treatment of the cloud droplet number concentration [*Ghan et al.*, 1997, 2000b; *Lohmann et al.*, 1999a] tend to produce reasonable results.

3.1.4. Further discussion of uncertainties. Some authors have argued that sea-salt particles may compete with sulphate aerosols as cloud condensation nuclei, thereby reducing the importance of anthropogenic sulphate in droplet nucleation [*O'Dowd et al.*, 1999; *Ghan et al.*, 1998]. While this process is accounted for in some of the above mentioned estimates, validation of its parameterizations against observations remains difficult, which adds further uncertainty. Considerable sensitivity is found to the parameterization of the autoconversion process [*Boucher et al.*, 1995; *Lohmann and Feichter*, 1997; *Jones et al.*, 1999], which complicates matters because there is a need to "tune" the autoconversion onset in GCMs [*Boucher et al.*, 1995; *Fowler et al.*, 1996; *Rotstayn*, 1999] to which the indirect aerosol forcing is sensitive [*Rotstayn*, 1999; *Jones et al.*, 1999; *Ghan et al.*, 2000a]. The indirect aerosol forcing is also sensitive to the treatment of the preindustrial aerosol concentrations and properties [*Jones et al.*, 1999; *Lohmann et al.*, 2000], which remains poorly characterized, the representation of the microphysics of midlevel clouds [*Lohmann et al.*, 2000], the representation of aerosol size distribution [*Ghan et al.*, 2000a], the parameterization of subgrid-scale clouds [*Ghan and Easter*, 1998], and the ability of GCMs to simulate the stratus and stratocumulus cloud fields. Also, it should be noted that all the studies discussed above cannot be considered as truly "independent" because many of them (with the exception of those of *Lohmann et al.* [2000] and *Ghan et al.* [2000a]) use similar methodologies and similar relationships between sulphate mass and cloud droplet number concentration. Therefore the range of results does not encompass the total range of uncertainties.

3.2. Other Aerosol Species

3.2.1. Carbonaceous aerosols. In this section, carbonaceous aerosols refer to the mixture (internal or external) of OC and BC aerosols. *Novakov and Penner* [1993] and *Novakov and Corrigan* [1996] have suggested that organic aerosols may act as efficient cloud condensation nuclei. There have been few GCM studies estimating the indirect forcing from carbonaceous aerosols. *Penner et al.* [1996] reported a range of forcing from -2.5 to -4.5 W m^{-2} (not reported in Table 4), which may be too large because of low natural emissions of organic aerosols and neglect of absorption of solar absorption by black carbon within the cloud. *Lohmann et al.* [2000] predicted a radiative impact for the combined effect (i.e., first and second effects) of -1.3 and -0.9 W m^{-2} for externally and internally mixed carbonaceous aerosols, respectively. These estimates do not include the effects of secondary organic aerosols or the effects of absorption of solar radiation by black carbon within the cloud.

3.2.2. Combination of sulphate and carbonaceous aerosols. *Lohmann et al.* [2000] found that the radiative impact of sulphate and carbonaceous aerosols considered simultaneously (-1.1 W m^{-2} for the internally mixed assumptions) is comparable to the sum of the radiative impacts calculated separately (-0.4 and -0.9 W m^{-2} for sulphate and carbonaceous aerosols, respectively). This finding is to be related to the fact that sulphate production does not form new particles in their model. Therefore this result probably does not hold for the other studies, and it is likely that the indirect radiative forcings by sulphate and carbonaceous aerosols computed independently do not add linearly. In fact, most of the GCM studies of the indirect aerosol effect used sulphate as a surrogate for the total anthropogenic fraction of the aerosol [e.g., *Boucher and Lohmann*, 1995; *Feichter et al.*, 1997; *Lohmann and Feichter*, 1997]. In this case the computed forcings incorporate the effects of other aerosol types that have a spatial distribution similar to sulphate aerosols, such as nitrate aerosols or carbonaceous aerosols from fossil fuel combustion. It does not include, however, the effects of biomass-burning aerosols, which have a spatial distribution different from sulphate aerosols.

Another issue is the potential for light-absorbing aerosols to increase in-cloud absorption of solar radiation (and correspondingly decrease the cloud albedo) when incorporated inside cloud droplets. This effect is generally not considered in the GCM studies, where the

black carbon is included as interstitial particles within the cloudy areas. *Twohy et al.* [1989] concluded from measurements off the coast of California and from simple radiative calculations that the observed levels of soot would not lead to a significant impact on the cloud albedo. *Chýlek et al.* [1996a] estimated an upper bound for increased absorption of solar radiation of 1–3 W m^{-2} (global and annual average) for a black carbon concentration of 0.5 μg m^{-3}. Considering the modeled atmospheric concentrations of soot (see sections 2.3.1 and 2.3.3) and the fact that only a small fraction of the soot is incorporated in the cloud droplets, the effect is probably smaller by 1–2 orders of magnitude. It remains, however, to be estimated properly. For instance, *Heintzenberg and Wendisch* [1996] showed that the decrease in radiative forcing due to a decrease in soot concentrations with increasing distance from the pollution sources could be compensated for by a concurrent increase in the fraction of soot which is incorporated in the cloud droplets.

3.2.3. Mineral dust aerosols. *Levin et al.* [1996] observed desert dust particles coated with sulphate. Such particles may originate from in-cloud scavenging of interstitial dust particles followed by evaporation of the cloud droplets (see also sections 2.6 and 2.8 for the direct effect). The presence of soluble material (which may be of anthropogenic origin) on the desert dust particles converts them into large and effective CCN, which may affect the cloud microphysics. Whether this effect results in a significant climate forcing has not been investigated and cannot presently be quantified.

3.2.4. Effect of gas phase nitric acid. *Kulmala et al.* [1993, 1995] argued that enhanced concentrations of condensable vapors (such as HNO_3 and HCl) in the atmosphere could affect cloud properties by facilitating the activation of cloud condensation nuclei. The impact of such an effect on the planetary cloud albedo has not been assessed.

3.3. Other Methods for Estimating the Indirect Aerosol Effect

3.3.1. The "missing" climate forcing. Hansen and colleagues have used two alternative approaches to characterize and quantify any "missing" climate forcings besides those due to greenhouse gases, solar constant, ozone, and aerosol direct effect. *Hansen et al.* [1995] used a simplified GCM to investigate the impact of various climate forcings on the diurnal cycle of surface air temperature. They found that although the aerosol direct effect or an increase in continental cloud albedo could contribute to damp the surface temperature diurnal cycle, only an increase in continental cloud cover would be consistent with observations [*Karl et al.*, 1993]. The required cloud increase depends on cloud height and would be of the order of 1% global coverage for low clouds (i.e., 2–5% over land). We cannot rule out that such a change is an unidentified cloud feedback rather than a forcing. *Hansen et al.* [1997b] also argued that agreement between observed and computed temperature trends requires the presence of another forcing of at least −1 W m^{-2}. However, this method assumes that the observed change in surface temperature since the preindustrial times is entirely a response to anthropogenic forcings, that all the other anthropogenic forcings are well quantified, and that the climate sensitivity parameter (see section 1) predicted by the GCM is correct. As outlined by *Rodhe et al.* [2000], there is also a risk of circular reasoning in estimating the indirect radiative forcing of aerosols in this manner. Therefore it may simply be a coincidence that such an estimate is consistent with the GCM estimates discussed above.

3.3.2. Remote sensing of the indirect effects of aerosols. Because of their global coverage, satellite observations are very useful to evaluate the results of general circulation models. They also provide some insights on the detection and quantification of the indirect radiative effects of aerosols on clouds. *Han et al.* [1994] analyzed AVHRR satellite radiances to retrieve the cloud droplet size of low-level clouds. They reported significant interhemispheric differences for both maritime and continental clouds. *Boucher* [1995] showed that if this difference is to be attributed to anthropogenic aerosols, it implied a differential forcing of about −1 W m^{-2} between the two hemispheres. Assuming a NH:SH ratio of 2:1 for the aerosol indirect effect, this would imply a globally averaged forcing of −1.5 W m^{-2}. Using an independent technique for retrieving cloud droplet size, *Bréon and Goloub* [1998] and *Bréon et al.* [1999] confirmed the smaller size of cloud droplets in the Northern Hemisphere compared with the Southern Hemisphere. They also noted smaller cloud droplet sizes downstream from the source regions of anthropogenic aerosols. The technique of *Bréon and Goloub* [1998] is based on the polarization signature of cloud droplets in the rainbow scattering angle, which requires specific conditions of observations and applies only to homogeneous cloud fields; therefore it is currently difficult to extrapolate these results to the global scale. In a recent analysis of the International Satellite Cloud Climatology Programme (ISCCP) data, *Han et al.* [1998a] revealed a more complicated picture. They found that the cloud albedo increases with decreasing cloud droplet size for most continental clouds and for all optically thick clouds. However, the cloud albedo is observed to decrease with decreasing droplet size for the optically thinner clouds over the oceans. Correlations between cloud albedo and cloud droplet size (or similarly, aerosol optical depth) are in fact not meaningful if they are not made for clouds that are comparable with respect to their other macroscopic properties such as geometrical thickness. In particular, this study underlines the limitations in using the hemispheric contrast in droplet size as an indicator of the aerosol indirect forcing, as was done by *Boucher* [1995]. In this context the positive correlation between aerosol optical depth and cloud optical depth and the

negative correlation between aerosol optical depth and cloud droplet size found by *Wetzel and Stowe* [1999] for stratus clouds have to be interpreted with caution.

Kaufman and Nakajima [1993] used AVHRR data to analyze bright warm clouds over Brazil during the biomass-burning season. While they found a decrease in the cloud droplet size, they also found a decrease in the cloud reflectance when the smoke optical thickness increased and accredited this to the effects of absorbing graphitic carbon particles within the cloud. *Kaufman and Fraser* [1997] used a similar approach to observe thinner and less reflective clouds. They showed that smoke reduced the cloud droplet size and increased the cloud reflectance for smoke optical depth up to 0.8. They estimated the indirect radiative forcing by smoke to be -2 W m^{-2} over this region for the 3 months of biomass burning, which would suggest a much smaller global average. However, using a combination of satellite observations and a global chemistry model, *Remer et al.* [1999] estimate that 50% of the cumulative biomass-burning aerosol indirect forcing occurs for smoke optical depth smaller than 0.1, that is, well away from the source regions.

Rosenfeld [1999, 2000] used a combination of AVHRR and Tropical Rainfall Measuring Mission (TRMM) satellite observations to investigate precipitation formation in clouds. He gave evidence for a suppression of precipitation in clouds locally affected by high levels of pollution from biomass burning or industrial aerosols. However, it seems to be currently difficult to quantify the cloud lifetime effect on the global scale from satellite measurements.

3.4. Aerosol Indirect Effect on Ice Clouds

3.4.1. Contrails and contrail-induced cloudiness. Contrails are ice clouds that form under some thermodynamical conditions after aircraft have passed in the upper troposphere. Their radiative effect is similar to that of thin cirrus clouds. Line-shaped contrails can be identified in satellite data, either from visual inspection [*Bakan et al.*, 1994] or through some automatic detection scheme [*Mannstein et al.*, 1999]. These studies indicate that line-shaped contrails have an average cover of between 0.5 and 2% in some parts of Europe and the eastern North Atlantic. Using meteorological and air traffic data scaled to regional observations of contrail cover, *Sausen et al.* [1998] estimated the present-day global mean cover by line-shaped contrails to be about 0.1%. This results in a global- and annual-mean radiative forcing by line-shaped contrails of 0.02 W m^{-2} [*Minnis et al.*, 1999], subject to an uncertainty factor of about 4, due to uncertainties in the contrail cover, optical depth, ice particle size, and shape [*Meerkötter et al.*, 1999].

When the ambient relative humidity exceeds ice saturation, contrails can evolve into extended cirrus clouds. *Boucher* [1999] and *Fahey et al.* [1999] have shown evidence that cirrus occurrence and coverage may have increased in regions of high air traffic compared with the rest of the globe. The trends in cirrus clouds could not be established with accuracy because of quantitative differences between the ground-based and satellite observations. *Smith et al.* [1998] reported the existence of nearly invisible layers of small ice crystals, which cause absorption of infrared radiation and could be due to remnant contrail particles. From consideration of the spatial distribution of cirrus trends during the last 25 years, *Fahey et al.* [1999] gave a range of 0 to 0.04 W m^{-2} for the radiative forcing due to aviation-induced cirrus. The available information on cirrus clouds was deemed insufficient to determine a single best estimate or an uncertainty range.

3.4.2. Impact of aircraft exhaust on cirrus cloud microphysics. Measurements by *Ström and Ohlsson* [1998] in a region of high air traffic revealed higher crystal number concentrations in areas of the cloud affected by soot emissions from aircraft. If the observed enhancement in crystal number density (which is about a factor of 2) is associated with a reduction in the mean crystal size, a change in cloud radiative forcing may result. *Wyser and Ström* [1998] estimated the forcing, although with considerable uncertainty, to be of the order of 0.3 W m^{-2} in regions of dense air traffic under the assumption of a 20% decrease of the mean crystal size. No estimate of the globally averaged radiative forcing is available.

Sedimentation of ice particles from contrails may remove water vapor from the upper troposphere. This effect is expected to be more important in strongly supersaturated air when ice particles can fall without evaporating [*Fahey et al.*, 1999]. The impacts of such an effect on cirrus formation, vertical profile of humidity, and the subsequent radiative forcing have not been assessed.

3.4.3. Effect of anthropogenic aerosols emitted at the surface on ice clouds. Aerosols also serve as ice nuclei, although it is well recognized that there are fewer ice nuclei than cloud condensation nuclei. It is conceivable that anthropogenic aerosols emitted at the surface and transported to the upper troposphere affect the formation and properties of ice clouds.

Jensen and Toon [1997] suggested that insoluble particles from the surface or soot particles emitted by aircraft, if sufficiently effective ice nuclei, can result in an increase in cirrus cloud coverage. *Laaksonen et al.* [1997] argued that nitric acid pollution is able to cause an increase in supercooled cirrus cloud droplet concentrations and thereby influence climate. Such effects, if significant at all, are not quantified at present.

4. SUMMARY AND CONCLUSION

Table 5 shows a summary of the range of radiative forcings for the direct and indirect effect of aerosols that

TABLE 5. A Summary of the Range of Radiative Forcings Discussed in the Text

Forcing Mechanism	*Aerosol Species*	*IPCC [1996], W m^{-2}*	*Range Discussed in the Text, W m^{-2}*	*Remarks*
Direct effect	sulphate aerosol	−0.2 to −0.8	−0.26 to −0.82	main uncertainties in column burden and effects of relative humidity and cloud
	fossil fuel BC	+0.03 to +0.3	+0.16 to +0.42	smallest estimates for an external mixture, largest estimates for an internal mixture
	fossil fuel OC	NA	−0.02 to −0.04	likely to be a lower limit due to the effects of mixing and unresolved hygroscopicity
	biomass-burning BC + OC	−0.07 to −0.6	−0.14 to −0.74	highest estimate has larger atmospheric burden and specific extinction coefficient
	mineral dust	NA	−0.46 to +0.09	significant positive terrestrial and negative solar radiative forcing lead to uncertainties in the sign of the radiative forcing
	nitrate aerosol	NA	−0.03	only one very tentative estimate available
Indirect effect	cloud albedo effect	−0 to −1.5	−0.3 to −1.8	this range for sulphate aerosols only
	cloud lifetime effect	NE	−0.4 to −2.3	this range for sulphate aerosols only[a]
	contrails	NA	0.005 to 0.06	this estimate based on *IPCC* [1999]
	aviation-induced cirrus	NA	0.04	this estimate based on *IPCC* [1999]; no range given

The range of radiative forcings from *IPCC* [1996] is included where appropriate. NA indicates that *IPCC* [1996] did not consider this forcing mechanism. NE indicates that *IPCC* [1996] did not give any estimate.

[a]GCM estimates cannot be strictly considered as radiative forcing calculations (see text).

have become available in the literature since *IPCC* [1996]. For sulphate aerosol the direct radiative forcing ranges from −0.26 W m^{-2} [*Graf et al.*, 1997] to −0.82 W m^{-2} [*Haywood and Ramaswamy*, 1998] and depends not just on the column burden determined by the chemical transport models, but also on the treatment of relative humidity and cloud. For fossil fuel BC aerosol the direct radiative forcing ranges from +0.16 to +0.42 W m^{-2} [*Myhre et al.*, 1998], the major factor influencing the radiative forcing being the degree of internal mixing. The two studies that have examined the radiative forcing due to fossil fuel OC lead to radiative forcings of −0.02 W m^{-2} [*Cooke et al.*, 1999] and −0.04 W m^{-2} [*Penner et al.*, 1998], although the forcing may be stronger if the effects of mixing and relative humidity are considered. Estimates of the radiative forcing due to OC and BC from biomass burning range from −0.14 W m^{-2} [*Penner et al.*, 1998] to −0.74 W m^{-2} [*Iacobellis et al.*, 1999]; the main uncertainties appear to be in the emission factors that subsequently affect the atmospheric burden of aerosol and the assumed optical parameters. For mineral dust, even the sign of the radiative forcing is in doubt due to the competing nature of the (negative) solar radiative forcing and (positive) terrestrial radiative forcing. Estimates of the radiative forcing due to mineral dust range from −0.46 W m^{-2} [*Sokolik and Toon*, 1996] to +0.09 W m^{-2} [*Tegen et al.*, 1996]. Areas of uncertainty in determining the radiative forcing due to mineral dust lie in determining the fraction that is of anthropogenic origin and determining the optical characteristics. Only one tentative estimate of the radiative forcing due to nitrate aerosol is available at −0.03 W m^{-2}. It should be noted that the overall direct effect of anthropogenic aerosols is unlikely to equal simply the sum of all of the individual radiative forcing components due to the complexities of internal mixing. Additionally, the range in the estimates in the literature makes it difficult to quantify the overall direct radiative forcing of aerosols. Satellite retrievals of aerosol radiative effects have made considerable progress in determining the radiative effects of aerosols over ocean regions provided they are carefully calibrated against field measurements. Satellite retrievals of the radiative effects over land currently remain problematic, as does determining the anthropogenic component of aerosols from satellite data.

For the indirect effect of aerosols, only GCM estimates of the cloud albedo effect computed in a diagnostic manner can be strictly compared against estimates of the radiative forcing by other agents (e.g., greenhouse gases). The GCM studies dedicated to the cloud lifetime effect (or second indirect effect) usually approximate its radiative impact as the change in top-of-atmosphere fluxes between two independent experiments (with and without aerosols), which may allow feedbacks on the hydrological cycle and the dynamics of the atmosphere to develop. The second indirect effect is therefore difficult to define and quantify in the context of current evaluations of radiative forcing of climate change and current model simulations. Nevertheless, available GCM simulations suggest a radiative flux perturbation for the second aerosol indirect effect of a magnitude similar to that for the first effect. Published GCM estimates of the radiative forcing for the cloud albedo effect by sulphate aerosols range from −0.3 to −1.8 W m^{-2}. GCM estimates of the radiative impact of the second indirect effect by sulphate aerosols range from −0.4 to −2.3 W

m^{-2}. Only one reliable GCM estimate of the effect of carbonaceous aerosols indicates a radiative impact of -0.9 W m^{-2} for the combined (first and second) effects. The aerosol indirect radiative forcing due to all aerosols differs significantly from the sum of the radiative forcings by the individual components. In particular, the indirect effects of sulphate and carbonaceous aerosols cannot be added up because of internal mixing and because the different aerosol species compete with each other to form cloud droplets. It is argued that present estimates of the indirect aerosol effects are subject to large uncertainties and that the present range of estimates does not necessarily reflect the actual uncertainty range because most GCMs use similar assumptions. Also, absorption of solar radiation by black carbon aerosols incorporated into the cloud droplets, although probably a second-order effect, is generally not considered in the GCM studies. Recent field campaigns (e.g., ACE 2) provided useful insights into the chemistry and physics of the aerosol indirect effects. It will be fruitful to "scale up" the observations at the local scale to the larger scale of the GCMs in order to evaluate and improve the parameterizations. Combined satellite retrievals of aerosol and cloud parameters are becoming useful tools to diagnose the radiative impact of the first indirect effect but require a careful interpretation. Global-scale satellite observations of cloud microphysical properties will also help to validate the GCM simulations of the aerosol indirect effects. Clearly, more research is needed regarding the indirect effects of aerosols, especially as far as middle- and high-level clouds are concerned.

These estimates for the aerosol direct and indirect effects derived from the published literature can be compared against a radiative forcing for well-mixed greenhouse gases of +2.45 W m^{-2} [*IPCC*, 1996]. We believe that the effects of aerosols continue to represent one of the largest uncertainties in the detection and prediction of climate change.

ACKNOWLEDGMENTS. C. Chuang, R. van Dorland, J. Feichter, H.-F. Graf, K. E. Grant, J. Hansen, J. Kiehl, Z. Kogan, G. Myhre, K. Restad, H. Rodhe, J. Roeckner, and L. Rotstayn are thanked for making their model results available. Special thanks are extended to Q. Han, S. Ghan, A. Jones, U. Lohmann, J. Penner, and I. Tegen for providing the data used in the figures. The authors are grateful to V. Ramaswamy and S. Solomon for encouragement in writing this review. This manuscript benefited from constructive comments by reviewers and D. L. Roberts.

Michael Coffey was the Editor responsible for this paper. He thanks J. Kiehl and an anonymous reviewer for the technical reviews and B. Scanlon for the cross-disciplinary review.

REFERENCES

Ackerman, S. A., Remote sensing aerosols using satellite infrared observations, *J. Geophys. Res.*, *102*, 17,069–17,079, 1997.

Ackerman, S. A., and H. Chung, Radiative effects of airborne dust on regional energy budgets at the top of the atmosphere, *J. Appl. Meteorol.*, *31*, 223–233, 1992.

Adams, P. J., J. H. Seinfeld, and D. M. Koch, Global concentrations of tropospheric sulfate, nitrate, and ammonium aerosol simulated in a general circulation model, *J. Geophys. Res.*, *104*, 13,791–13,823, 1999.

Albrecht, B. A., Aerosols, cloud microphysics, and fractional cloudiness, *Science*, *245*, 1227–1230, 1989.

Bakan, S., M. Betancor, V. Gayler, and H. Grassl, Contrail frequency over Europe from NOAA-satellite images, *Ann. Geophys.*, *12*, 962–968, 1994.

Barth, M. C., P. J. Rasch, J. T. Kiehl, C. M. Benkovitz, and S. E. Schwartz, Sulfur chemistry in the National Center for Atmospheric Research Community Climate Model: Description, evaluation, features, and sensitivity to aqueous chemistry, *J. Geophys. Res.*, *105*, 1387–1415, 2000.

Benkovitz, C. M., M. T. Scholtz, J. Pacyna, L. Tarrason, J. Dignon, E. C. Voldner, P. A. Spiro, J. A. Logan, and T. E. Graedel, Global gridded inventories of anthropogenic emissions of sulfur and nitrogen, *J. Geophys. Res.*, *101*, 29,239–29,253, 1996.

Boucher, O., GCM estimate of the indirect aerosol forcing using satellite-retrieved cloud effective droplet radii, *J. Clim.*, *8*, 1403–1409, 1995.

Boucher, O., Aircraft can increase cirrus cloudiness, *Nature*, *397*, 30–31, 1999.

Boucher, O., and T. L. Anderson, General circulation model assessment of the sensitivity of direct climate forcing by anthropogenic sulfate aerosols to aerosol size and chemistry, *J. Geophys. Res.*, *100*, 26,117–26,134, 1995.

Boucher, O., and U. Lohmann, The sulfate-CCN-cloud albedo effect: A sensitivity study using two general circulation models, *Tellus*, *Ser. B*, *47*, 281–300, 1995.

Boucher, O., and H. Rodhe, The sulfate-CCN-cloud albedo effect: A sensitivity study, *Rep. CM-83*, 20 pp., Dep. of Meteorol., Stockholm Univ., Stockholm, 1994.

Boucher, O., and D. Tanré, Estimation of the aerosol perturbation to the Earth's radiative budget over the oceans using POLDER satellite aerosol retrievals, *Geophys. Res. Lett.*, *27*, 1103–1106, 2000.

Boucher, O., H. Le Treut, and M. B. Baker, Precipitation and radiation modeling in a general circulation model: Introduction of cloud microphysics, *J. Geophys. Res.*, *100*, 16,395–16,414, 1995.

Boucher, O., et al., Intercomparison of models representing direct shortwave radiative forcing by sulfate aerosols, *J. Geophys. Res.*, *103*, 16,979–16,998, 1998.

Brenguier, J.-L., P. Y. Chuang, Y. Fouquart, D. W. Johnson, F. Parol, H. Pawlowska, J. Pelon, L. Schüller, F. Schröder, and J. Snider, An overview of the ACE-2 CloudyColumn Closure Experiment, *Tellus*, *Ser. B*, *52*, 815–827, 2000a.

Brenguier, J.-L., H. Pawlowska, L. Schüller, R. Preusker, J. Fischer, and Y. Fouquart, Radiative properties of boundary layer clouds: Droplet effective radius versus number concentration, *J. Atmos. Sci.*, *57*, 803–821, 2000b.

Bréon, F.-M., and P. Goloub, Cloud droplet effective radius from spaceborne polarization measurements, *Geophys. Res. Lett.*, *25*, 1879–1882, 1998.

Bréon, F.-M., S. Colzy, and P. Goloub, Global distribution of cloud droplet radius from POLDER polarization measurements, in *Proceedings of the ALPS99 International Conference, 18–22 January 1999, Méribel, France*, pp. WK1 and WK2/O/08/1–4, Cent. Natl. des Etudes Spatiales, Toulouse, France, 1999.

Capaldo, K., J. J. Corbett, P. Kasibhatla, P. Fischbeck, and S. N. Pandis, Effects of ship emissions on sulphur cycling and radiative climate forcing over the ocean, *Nature*, *400*, 743–746, 1999.

Charlson, R. J., S. E. Schwartz, J. M. Hales, R. D. Cess, J. A. Coakley, J. E. Hansen, and D. J. Hofmann, Climate forcing by anthropogenic aerosols, *Science*, *255*, 423–430, 1992.

Charlson, R. J., T. L. Anderson, and H. Rodhe, Direct climate forcing by anthropogenic aerosols: Quantifying the link between sulfate and radiation, *Contrib. Atmos. Phys.*, *72*, 79–94, 1999.

Chin, M., and D. J. Jacob, Anthropogenic and natural contributions to tropospheric sulfate: A global model analysis, *J. Geophys. Res.*, *101*, 18,691–18,699, 1996.

Chuang, C. C., J. E. Penner, K. E. Taylor, and J. J. Walton, Climate effects of anthropogenic sulfate: Simulation from a coupled chemistry/climate model, in *Preprints of the AMS Conference on Atmospheric Chemistry*, pp. 170–174, Am. Meteorol. Soc., Boston, Mass., 1994.

Chuang, C. C., J. E. Penner, K. E. Taylor, A. S. Grossman, and J. J. Walton, An assessment of the radiative effects of anthropogenic sulfate, *J. Geophys. Res.*, *102*, 3761–3778, 1997.

Chýlek, P., and J. Wong, Effect of absorbing aerosols on global radiation budget, *Geophys. Res. Lett.*, *22*, 929–931, 1995.

Chýlek, P., G. Videen, and D. Ngo, Effect of black carbon on the optical properties and climate forcing of sulfate aerosols, *J. Geophys. Res.*, *100*, 16,325–16,332, 1995.

Chýlek, P., C. M. Banic, B. Johnson, P. A. Damiano, G. A. Isaac, W. R. Leaitch, P. S. K. Liu, F. S. Boudala, B. Winter, and D. Ngo, Black carbon: Atmospheric concentrations and cloud water content measurements over southern Nova Scotia, *J. Geophys. Res.*, *101*, 29,105–29,110, 1996a.

Chýlek, P., G. B. Lesins, G. Videen, J. G. D. Wong, R. G. Pinnick, D. Ngo, and J. D. Klett, Black carbon and absorption of solar radiation by clouds, *J. Geophys. Res.*, *101*, 23,365–23,371, 1996b.

Claquin, T., M. Schulz, Y. Balkanski, and O. Boucher, Uncertainties in assessing radiative forcing by mineral dust, *Tellus*, *Ser. B*, *50*, 491–505, 1998.

Claquin, T., M. Schulz, and Y. Balkanski, Modeling the mineralogy of atmospheric dust sources, *J. Geophys. Res.*, *104*, 22,243–22,256, 1999.

Coakley, J. A., Jr., R. L. Bernstein, and P. A. Durkee, Effect of ship-stack effluents on cloud reflectivity, *Science*, *237*, 1020–1022, 1987.

Cooke, W. F., and J. J. N. Wilson, A global black carbon model, *J. Geophys. Res.*, *101*, 19,395–19,409, 1996.

Cooke, W. F., C. Liousse, H. Cachier, and J. Feichter, Construction of a 1° × 1° fossil fuel emission data set for carbonaceous aerosol and implementation and radiative impact in the ECHAM4 model, *J. Geophys. Res.*, *104*, 22,137–22,162, 1999.

Cox, S. J., W.-C. Wang, and S. E. Schwartz, Climate response to radiative forcings by aerosols and greenhouse gases, *Geophys. Res. Lett.*, *22*, 2509–2512, 1995.

Cusack, S., A. Slingo, J. M. Edwards, and M. Wild, The radiative impact of a simple aerosol climatology on the Hadley Centre atmospheric GCM, *Q. J. R. Meteorol. Soc.*, *124*, 2517–2526, 1998.

Dentener, F. J., G. R. Carmichael, Y. Zhang, J. Lelieveld, and P. Crutzen, Role of mineral aerosol as a reactive surface in the global troposphere, *J. Geophys. Res.*, *101*, 22,869–22,889, 1996.

Deuzé, J.-L., M. Herman, P. Goloub, D. Tanré, and A. Marchand, Characterization of aerosols over the ocean from POLDER/ADEOS-1, *Geophys. Res. Lett.*, *26*, 1421–1424, 1999.

Dubovik, O., B. N. Holben, Y. N. Kaufman, M. Yamasoe, A. Smirnov, D. Tanré, and I. Slutsker, Single-scattering albedo of smoke retrieved from the sky radiance and solar transmittance measured from ground, *J. Geophys. Res.*, *103*, 31,903–31923, 1998.

Eck, T. F., B. N. Holben, I. Slutsker, and A. Setzer, Measurements of irradiance attenuation and estimation of aerosol single scattering albedo for biomass burning aerosols in Amazonia, *J. Geophys. Res.*, *103*, 31,865–31,878, 1998.

Fahey, D. W., U. Schumann, S. Ackerman, P. Artaxo, O. Boucher, M. Y. Danilin, B. Kärcher, P. Minnis, T. Nakajima, and O. B. Toon, Aviation-produced aerosols and cloudiness, in *Aviation and the Global Atmosphere*, edited by J. E. Penner et al., chap. 3, pp. 65–120, Cambridge Univ. Press, New York, 1999.

Feichter, J., U. Lohmann, and I. Schult, The atmospheric sulfur cycle in ECHAM-4 and its impact on the shortwave radiation, *Clim. Dyn.*, *13*, 235–246, 1997.

Flowerdew, R. J., and J. D. Haigh, Retrieval of aerosol optical thickness over land using the ATSR-2 dual-look satellite radiometer, *Geophys. Res. Lett.*, *23*, 351–354, 1996.

Fowler, L. D., D. A. Randall, and S. A. Rutledge, Liquid and ice cloud microphysics in the CSU general circulation model, part I, Model description and simulated microphysical processes, *J. Clim.*, *9*, 489–529, 1996.

Francis, P. N., P. Hignett, and J. P. Taylor, Aircraft observations and modeling of sky radiance distributions from aerosol during TARFOX, *J. Geophys. Res.*, *104*, 2309–2319, 1999.

Ghan, S., and R. Easter, Comment on "A limited-area-model case study of the effects of sub-grid scale variations in relative humidity and cloud upon the direct radiative forcing of sulfate aerosol" by Haywood et al., *Geophys. Res. Lett.*, *25*, 1039–1040, 1998.

Ghan, S. J., and J. E. Penner, Smoke: Effects on climate, in *Encyclopedia of Earth System Science*, vol. 4, edited by W. A. Nierenberg, pp. 191–198, Academic, San Diego, Calif., 1992.

Ghan, S. J., L. R. Leung, R. C. Easter, and H. Abdul-Razzak, Prediction of cloud droplet number in a general circulation model, *J. Geophys. Res.*, *102*, 21,777–21,794, 1997.

Ghan, S. J., G. Guzman, and H. Abdul-Razzak, Competition between sea salt and sulfate particles as cloud condensation nuclei, *J. Atmos. Sci.*, *55*, 3340–3347, 1998.

Ghan, S. J., R. C. Easter, E. Chapman, H. Abdul-Razzak, Y. Zhang, R. Leung, N. Laulainen, R. Saylor, and R. Zaveri, A physically based estimate of radiative forcing by anthropogenic sulfate aerosol, *J. Geophys. Res.*, in press, 2000a.

Ghan, S. J., N. Laulainen, R. Easter, R. Wagener, S. Nemesure, E. Chapman, Y. Zhang, and R. Leung, Evaluation of aerosol indirect radiative forcing in MIRAGE, *J. Geophys. Res.*, in press, 2000b.

Goloub, P., D. Tanré, J.-L. Deuzé, M. Herman, A. Marchand, and F.-M. Bréon, Validation of the first algorithm applied for deriving the aerosol properties over the ocean using the POLDER/ADEOS measurements, *IEEE Trans. Geosci. Remote Sens.*, *37*, 1586–1596, 1999.

Graf, H.-F., J. Feichter, and B. Langmann, Volcanic sulfur emissions: Estimates of source strength and its contribution to the global sulfate distribution, *J. Geophys. Res.*, *102*, 10,727–10,738, 1997.

Grant, K. E., C. C. Chuang, A. S. Grossman, and J. E. Penner, Modeling the spectral optical properties of ammonium sulfate and biomass burning aerosols: Parameterization of relative humidity effects and model results, *Atmos. Environ.*, *33*, 2603–2620, 1999.

Han, Q., W. B. Rossow, and A. A. Lacis, Near-global survey of effective droplet radii in liquid water clouds using ISCCP data, *J. Clim.*, *7*, 465–497, 1994.

Han, Q., W. B. Rossow, J. Chou, and R. M. Welch, Global survey of the relationships of cloud albedo and liquid water path with droplet size using ISCCP, *J. Clim.*, *11*, 1516–1528, 1998a.

Han, Q., W. B. Rossow, J. Chou, and R. M. Welch, Global

variation of column droplet concentration in low-level clouds, *Geophys. Res. Lett.*, *25*, 1419–1422, 1998b.

Hansen, J., D. Johnson, A. Lacis, S. Lebedeff, P. Lee, D. Rind, and G. Russell, Climate impact of increasing atmospheric carbon dioxide, *Science*, *213*, 957–966, 1981.

Hansen, J. E., M. Sato, and R. Ruedy, Long-term changes of the diurnal temperature cycle: Implications about mechanisms of global climate change, *Atmos. Res.*, *37*, 175–209, 1995.

Hansen, J., M. Sato, A. Lacis, and R. Ruedy, The missing climate forcing, *Philos. Trans. R. Soc. London, Ser. B*, *352*, 231–240, 1997a.

Hansen, J., M. Sato, and R. Ruedy, Radiative forcing and climate response, *J. Geophys. Res.*, *102*, 6831–6864, 1997b.

Hansen, J., M. Sato, A. Lacis, R. Ruedy, I. Tegen, and E. Matthews, Climate forcings in the industrial era, *Proc. Natl. Acad. Sci.*, *95*, 12,753–12,758, 1998.

Haywood, J. M., and V. Ramaswamy, Global sensitivity studies of the direct radiative forcing due to anthropogenic sulfate and black carbon aerosols, *J. Geophys. Res.*, *103*, 6043–6058, 1998.

Haywood, J. M., and K. P. Shine, The effect of anthropogenic sulfate and soot on the clear-sky planetary radiation budget, *Geophys. Res. Lett.*, *22*, 603–606, 1995.

Haywood, J. M., and K. P. Shine, Multi-spectral calculations of the radiative forcing of tropospheric sulphate and soot aerosols using a column model, *Q. J. R. Meteorol. Soc.*, *123*, 1907–1930, 1997.

Haywood, J. M., D. L. Roberts, A. Slingo, J. M. Edwards, and K. P. Shine, General circulation model calculations of the direct radiative forcing by anthropogenic sulphate and fossil-fuel soot aerosol, *J. Clim.*, *10*, 1562–1577, 1997a.

Haywood, J. M., V. Ramaswamy, and L. J. Donner, A limited-area-model case study of the effects of sub-grid scale variations in relative humidity and cloud upon the direct radiative forcing of sulfate aerosol, *Geophys. Res. Lett.*, *24*, 143–146, 1997b.

Haywood, J. M., V. Ramaswamy, and L. J. Donner, Reply, *Geophys. Res. Lett.*, *25*, 1041, 1998.

Haywood, J. M., V. Ramaswamy, and B. J. Soden, Tropospheric aerosol climate forcing in clear-sky satellite observations over the oceans, *Science*, *283*, 1299–1303, 1999.

Haywood, J. M., P. N. Francis, M. D. Glew, and J. P. Taylor, Optical properties and direct radiative effect of Saharan dust: A case study of two Saharan dust outbreaks using data from the U.K. Meteorological Office C-130, *J. Geophys. Res.*, in press, 2000.

Hegg, D. A., R. J. Ferek, and P. V. Hobbs, Light scattering and cloud condensation nucleus activity of sulfate aerosol measured over the northeastern Atlantic Ocean, *J. Geophys. Res.*, *98*, 14,887–14,894, 1993.

Hegg, D. A., J. Livingston, P. V. Hobbs, T. Novakov, and P. Russell, Chemical apportionment of aerosol column optical depth off the mid-Atlantic coast of the United States, *J. Geophys. Res.*, *102*, 25,293–25,303, 1997.

Heintzenberg, J., and M. Wendisch, On the sensitivity of cloud albedo to the partitioning of particulate absorbers in cloudy air, *Contrib. Atmos. Phys.*, *69*, 491–499, 1996.

Herman, J. R., P. K. Barthia, O. Torres, C. Hsu, C. Seftor, and E. Celarier, Global distribution of UV-absorbing aerosols from NIMBUS-7/TOMS data, *J. Geophys. Res.*, *102*, 16,911–16,922, 1997.

Herman, M., J.-L. Deuzé, C. Devaux, P. Goloub, F.-M. Bréon, and D. Tanré, Remote sensing of aerosols over land surfaces including polarization measurements and application to POLDER measurements, *J. Geophys. Res.*, *102*, 17,039–17,049, 1997.

Hignett, P., J. T. Taylor, P. N. Francis, and M. D. Glew, Comparison of observed and modeled direct aerosol forcing during TARFOX, *J. Geophys. Res.*, *104*, 2279–2287, 1999.

Higurashi, A., and T. Nakajima, Development of a two-channel aerosol retrieval algorithm on global scale using NOAA/AVHRR, *J. Atmos. Sci.*, *56*, 924–941, 1999.

Hobbs, P. V., J. S. Reid, R. A. Kotchenruther, R. J. Ferek, and R. Weiss, Direct radiative forcing by smoke from biomass burning, *Science*, *275*, 1776–1778, 1997.

Holben, B. N., et al., AERONET: A federated instrument network and data archive for aerosol characterization, *Remote Sens. Environ.*, *66*, 1–16, 1998.

Horvath, H., Atmospheric light absorption—A review, *Atmos. Environ., Part A*, *27*, 293–317, 1993.

Husar, R. B., J. M. Prospero, and L. L. Stowe, Characterization of tropospheric aerosols over the oceans with the NOAA advanced very high resolution radiometer optical thickness operational product, *J. Geophys. Res.*, *102*, 16,889–16,909, 1997.

Iacobellis, S. F., R. Frouin, and R. C. J. Somerville, Direct climate forcing by biomass-burning aerosols: Impact of correlations between controlling variables, *J. Geophys. Res.*, *104*, 12,031–12,045, 1999.

Intergovernmental Panel on Climate Change, *Climate Change 1994: Radiative Forcing of Climate Change and an Evaluation of the IPCC IS92 Emission Scenarios*, edited by J. T. Houghton et al., Cambridge Univ. Press, New York, 1994.

Intergovernmental Panel on Climate Change, *Climate Change 1995: The Science of Climate Change, The Contribution of Working Group I to the Second Assessment Report of the IPCC*, edited by J. T. Houghton et al., 572 pp., Cambridge Univ. Press, New York, 1996.

Intergovernmental Panel on Climate Change, *Aviation and the Global Atmosphere*, edited by J. E. Penner et al., 373 pp., Cambridge Univ. Press, New York, 1999.

Jankowiak, I., and D. Tanré, Satellite climatology of Saharan dust outbreaks: Method and preliminary results, *J. Clim.*, *5*, 646–656, 1992.

Jensen, E. J., and O. B. Toon, The potential impact of soot from aircraft exhaust on cirrus clouds, *Geophys. Res. Lett.*, *24*, 249–252, 1997.

Jones, A., and A. Slingo, Predicting cloud-droplet effective radius and indirect sulphate aerosol forcing using a general circulation model, *Q. J. R. Meteorol. Soc.*, *122*, 1573–1595, 1996.

Jones, A., and A. Slingo, Climate model studies of sulphate aerosols and clouds, *Philos. Trans. R. Soc. London, Ser. B*, *352*, 221–229, 1997.

Jones, A., D. L. Roberts, and A. Slingo, A climate model study of the indirect radiative forcing by anthropogenic sulphate aerosols, *Nature*, *370*, 450–453, 1994.

Jones, A., D. L. Roberts, and M. J. Woodage, The indirect effects of anthropogenic sulphate aerosol simulated using a climate model with an interactive sulphur cycle, *Tech. Note 14*, 38 pp., Hadley Cent., U.K. Meteorol. Off., Bracknell, England, 1999.

Karl, T. R., P. D. Jones, R. W. Knight, G. Kukla, N. Plummer, V. Razuvayev, K. P. Gallo, J. Lindseay, R. J. Charlson, and T. C. Peterson, A new perspective on recent global warming: Asymmetric trends of daily maximum and minimum temperature, *Bull. Am. Meteorol. Soc.*, *74*, 1007–1023, 1993.

Kasibhatla, P., W. L. Chameides, and J. St. John, A three-dimensional global model investigation of the seasonal variation in the atmospheric burden of anthropogenic sulfate aerosols, *J. Geophys. Res.*, *102*, 3737–3759, 1997.

Kattenberg, A., F. Giorgi, H. Grassl, G. A. Meehl, J. F. B. Mitchell, R. J. Stouffer, T. Tokioka, A. J. Weaver, and T. M. L. Wigley, Climate Models—Projections of Future Climate, in *Climate Change 1995: The Science of Climate Change, The Contribution of Working Group I to the Second*

Assessment Report of the IPCC, edited by J. T. Houghton et al., pp. 285–357, Cambridge Univ. Press, New York, 1996.

Kaufman, Y. J., Satellite sensing of aerosol absorption, *J. Geophys. Res.*, *92*, 4307–4317, 1987.

Kaufman, Y. J., and R. S. Fraser, Control of the effect of smoke particles on clouds and climate by water vapor, *Science*, *277*, 1636–1639, 1997.

Kaufman, Y. J., and T. Nakajima, Effect of Amazon smoke on cloud microphysics and albedo—Analysis from satellite imagery, *J. Appl. Meteorol.*, *32*, 729–744, 1993.

Kaufman, Y. J., D. Tanré, L. Remer, E. Vermote, A. Chu, and B. N. Holben, Operational remote sensing of tropospheric aerosol over land from EOS moderate resolution imaging spectroradiometer, *J. Geophys. Res.*, *102*, 17,051–17,067, 1997.

Kiehl, J. T., and B. P. Briegleb, The relative roles of sulfate aerosols and greenhouse gases in climate forcing, *Science*, *260*, 311–314, 1993.

Kiehl, J. T., and H. Rodhe, Modeling geographical and seasonal forcing due to aerosols, in *Aerosol Forcing of Climate*, pp. 281–296, edited by R. J. Charlson and J. Heintzenberg, John Wiley, New York, 1995.

Kiehl, J. T., T. L. Schneider, P. J. Rasch, M. C. Barth, and J. Wong, Radiative forcing due to sulfate aerosols from simulations with the National Center for Atmospheric Research Community Climate Model, Version 3, *J. Geophys. Res.*, *105*, 1441–1457, 2000.

King, M. D., Y. J. Kaufman, W. P. Menzel, and D. Tanré, Remote sensing of cloud, aerosol, and water vapor properties from the moderate resolution imaging spectrometer (MODIS), *IEEE Trans. Geosci. Remote Sens.*, *30*, 2–27, 1992.

King, M. D., Y. J. Kaufman, D. Tanré, and T. Nakajima, Remote sensing of tropospheric aerosols: Past, present, and future, *Bull. Am. Meteorol. Soc.*, *80*, 2229–2259, 1999.

Kirkevåg, A., T. Iversen, and A. Dahlback, On radiative effects of black carbon and sulphate aerosols, *Atmos. Environ.*, *33*, 2621–2635, 1999.

Koch, D., D. Jacob, I. Tegen, D. Rind, and M. Chin, Tropospheric sulfur simulation and sulfate direct radiative forcing in the Goddard Institute for Space Studies general circulation model, *J. Geophys. Res.*, *104*, 23,799–23,822, 1999.

Kogan, Z. N., Y. L. Kogan, and D. K. Lilly, Evaluation of sulfate aerosols indirect effect in marine stratocumulus clouds using observation-derived cloud climatology, *Geophys. Res. Lett.*, *23*, 1937–1940, 1996.

Kogan, Z. N., Y. L. Kogan, and D. K. Lilly, Cloud factor and seasonality of the indirect effect of anthropogenic sulfate aerosols, *J. Geophys. Res.*, *102*, 25,927–25,939, 1997.

Kotchenruther, R. A., P. V. Hobbs, and D. A. Hegg, Humidification factors for atmospheric aerosols off the mid-Atlantic coast of the United States, *J. Geophys. Res.*, *104*, 2239–2251, 1999.

Kulmala, M., A. Laaksonen, P. Korhonen, T. Vesala, and T. Ahonen, The effect of atmospheric nitric acid vapor on cloud condensation nucleus activation, *J. Geophys. Res.*, *98*, 22,949–22,958, 1993.

Kulmala, M., P. Korhonen, A. Laaksonen, and T. Vesala, Changes in cloud properties due to NO_x emissions, *Geophys. Res. Lett.*, *22*, 239–242, 1995.

Laaksonen, A., J. Hienola, M. Kulmala, and F. Arnold, Supercooled cirrus cloud formation modified by nitric acid pollution of the upper troposphere, *Geophys. Res. Lett.*, *24*, 3009–3012, 1997.

Langner, J., and H. Rodhe, A global three-dimensional model of the tropospheric sulfur cycle, *J. Atmos. Chem.*, *13*, 225–263, 1991.

Leaitch, W. R., G. A. Isaac, J. W. Strapp, C. M. Banic, and H. A. Wiebe, The relationship between cloud droplet number concentrations and anthropogenic pollution: Observations and climatic implications, *J. Geophys. Res.*, *97*, 2463–2474, 1992.

Legrand, M., J.-J. Bertrand, M. Desbois, L. Menenger, and Y. Fouquart, The potential of infrared satellite data for the retrieval of Saharan dust optical depth over Africa, *J. Appl. Meteorol.*, *28*, 309–318, 1989.

Leroy, M., J.-L. Deuzé, F.-M. Bréon, O. Hautecoeur, M. Herman, J.-C. Buriez, D. Tanré, S. Bouffiès, P. Chazette, and J. L. Roujean, Retrieval of atmospheric properties and surface bidirectional reflectances over land from POLDER/ADEOS, *J. Geophys. Res.*, *102*, 17,023–17,037, 1997.

Le Treut, H., M. Forichon, O. Boucher, and Z. X. Li, Sulfate aerosol indirect effect and CO_2 greenhouse forcing: Equilibrium response of the LMD GCM and associated cloud feedbacks, *J. Clim.*, *11*, 1673–1684, 1998.

Levin, Z., E. Ganor, and V. Gladstein, The effects of desert particles coated with sulfate on rain formation in the eastern Mediterranean, *J. Appl. Meteorol.*, *35*, 1511–1523, 1996.

Li, Z., and L. Kou, The direct radiative effect of smoke aerosols on atmospheric absorption of visible light, *Tellus, Ser. B*, *50*, 543–554, 1998.

Liao, H., and J. H. Seinfeld, Effect of clouds on direct radiative forcing of climate, *J. Geophys. Res.*, *103*, 3781–3788, 1998.

Liousse, C., H. Cachier, and S. G. Jennings, Optical and thermal measurements of black carbon content in different environments: Variation of specific attenuation cross-section, σ, *Atmos. Environ., Part A*, *27*, 1203–1211, 1993.

Liousse, C., J. E. Penner, C. C. Chuang, J. J. Walton, and H. Eddleman, A global three-dimensional model study of carbonaceous aerosols, *J. Geophys. Res.*, *101*, 19,411–19,432, 1996.

Lohmann, U., and J. Feichter, Impact of sulfate aerosols on albedo and lifetime of clouds: A sensitivity study with the ECHAM4 general circulation model, *J. Geophys. Res.*, *102*, 13,685–13,700, 1997.

Lohmann, U., J. Feichter, C. C. Chuang, and J. E. Penner, Prediction of the number of cloud droplets in the ECHAM general circulation model, *J. Geophys. Res.*, *104*, 9169–9198, 1999a. (Correction, *J. Geophys. Res.*, *104*, 24,557–24,563, 1999.)

Lohmann, U., K. von Salzen, N. McFarlane, H. G. Leighton, and J. Feichter, Tropospheric sulfur cycle in the Canadian general circulation model, *J. Geophys. Res.*, *104*, 26,833–26,858, 1999b.

Lohmann, U., J. Feichter, J. Penner, and R. Leaitch, Indirect effect of sulfate and carbonaceous aerosols: A mechanistic treatment, *J. Geophys. Res.*, *105*, 12,193–12,206, 2000.

Manabe, S., and R. T. Wetherald, Thermal equilibrium of the atmosphere with a given distribution of relative humidity, *J. Atmos. Sci.*, *24*, 241–259, 1967.

Mannstein, H., R. Meyer, and P. Wendling, Operational detection of contrails from NOAA-AVHRR data, *Int. J. Remote Sens.*, *20*, 1641–1660, 1999.

Martin, G. M., D. W. Johnson, and A. Spice, The measurement and parameterization of effective radius of droplets in warm stratiform clouds, *J. Atmos. Sci.*, *51*, 1823–1842, 1994.

Martins, J. V., P. V. Hobbs, R. E. Weiss, and P. Artaxo, Sphericity and morphology of smoke particles from biomass burning in Brazil, *J. Geophys. Res.*, *103*, 32,051–32,067, 1998.

McInnes, L. M., M. H. Bergin, J. A. Ogren, and S. Schwartz, Apportionment of light scattering and hygroscopic growth to aerosol composition, *Geophys. Res. Lett.*, *25*, 513–516, 1998.

Meerkötter, R., U. Schumann, D. R. Doelling, P. Minnis, T. Nakajima, and Y. Tsushima, Radiative forcing by contrails, *Ann. Geophys.*, *17*, 1080–1094, 1999.

Miller, R., and I. Tegen, Climate response to soil dust aerosols, *J. Clim.*, *11*, 3247–3267, 1998.

Miller, R., and I. Tegen, Radiative forcing of a tropical direct circulation by soil dust aerosols, *J. Atmos. Sci.*, *56*, 2403–2433, 1999.

Minnis, P., U. Schumann, D. R. Doelling, K. M. Gierens, and D. W. Fahey, Global distribution of contrail radiative forcing, *Geophys. Res. Lett.*, *26*, 1853–1856, 1999.

Mishchenko, M. I., L. D. Travis, R. A. Kahn, and R. A. West, Modeling phase functions for dustlike tropospheric aerosols using a shape mixture of randomly orientated polydisperse spheroids, *J. Geophys. Res.*, *102*, 16,831–16,847, 1997.

Moulin, C., F. Guillard, F. Dulac, and C. E. Lambert, Long-term daily monitoring of Saharan dust load over ocean using Meteosat ISCCP-B2 data, 1, Methodology and preliminary results for 1983–1994 in the Mediterranean, *J. Geophys. Res.*, *102*, 16,947–16,958, 1997.

Murphy, D. M., J. R. Anderson, P. K. Quinn, L. M. McInnes, M. Posfai, D. S. Thomson, and P. R. Buseck, Influence of sea-salt on aerosol radiative properties in the Southern Ocean marine boundary layer, *Nature*, *392*, 62–65, 1998.

Myhre, G., and F. Stordal, Global sensitivity experiments of the radiative forcing due to mineral aerosols, *J. Geophys. Res.*, in press, 2000.

Myhre, G., F. Stordal, K. Restad, and I. Isaksen, Estimates of the direct radiative forcing due to sulfate and soot aerosols, *Tellus, Ser. B*, *50*, 463–477, 1998.

Nakajima, T., and A. Higurashi, A use of two-channel radiances for aerosol characterization from space, *Geophys. Res. Lett.*, *25*, 3815–3818, 1998.

Nakajima, T., A. Higurashi, K. Aoki, T. Endoh, H. Fukushima, M. Toranti, Y. Mitomi, B. G. Mitchell, and R. Frouin, Early phase analysis of OCTS radiance data for aerosol remote sensing, *IEEE Trans. Geosci. Remote Sens.*, *37*, 1575–1585, 1999.

Nemesure, S., R. Wagener, and S. E. Schwartz, Direct shortwave forcing of climate by anthropogenic sulfate aerosol: Sensitivity to particle size, composition, and relative humidity, *J. Geophys. Res.*, *100*, 26,105–26,116, 1995.

Novakov, T., and C. E. Corrigan, Cloud condensation nucleus activity of the organic component of biomass smoke particles, *Geophys. Res. Lett.*, *23*, 2141–2144, 1996.

Novakov, T., and J. E. Penner, Large contribution of organic aerosols to cloud-condensation-nuclei concentrations, *Nature*, *365*, 823–826, 1993.

Novakov, T., C. Rivera-Carpio, J. E. Penner, and C. F. Rogers, The effect of anthropogenic sulfate aerosols on marine cloud droplet concentrations, *Tellus, Ser. B*, *46*, 132–141, 1994.

Novakov, T., D. A. Hegg, and P. V. Hobbs, Airborne measurements of carbonaceous aerosols during TARFOX, *J. Geophys. Res.*, *102*, 30,023–30,030, 1997.

O'Dowd, D., J. A. Lowe, and M. H. Smith, Coupling sea-salt and sulphate interactions and its impact on cloud droplet concentration predictions, *Geophys. Res. Lett.*, *26*, 1311–1314, 1999.

Pan, W., M. A. Tatang, G. J. McRae, and R. T. G. Prinn, Uncertainty analysis of the direct radiative forcing by anthropogenic sulfate aerosols, *J. Geophys. Res.*, *102*, 21,915–21,924, 1997.

Penner, J. E., R. E. Dickinson, and C. A. O'Neill, Effects of aerosol from biomass burning on the global radiation budget, *Science*, *256*, 1432–1434, 1992.

Penner, J. E., H. Eddleman, and T. Novakov, Towards the development of a global inventory for black carbon emissions, *Atmos. Environ., Part A*, *27*, 1277–1295, 1993.

Penner, J. E., R. J. Charlson, J. M. Hales, N. S. Laulainen, R. Leifer, T. Novakov, J. Ogren, L. F. Radke, S. E. Schwartz, and L. Travis, Quantifying and minimising uncertainty of climate forcing by anthropogenic aerosols, *Bull. Am. Meteorol. Soc.*, *75*, 375–400, 1994.

Penner, J. E., C. C. Chuang, and C. Liousse, The contribution of carbonaceous aerosols to climate change, in *Nucleation and Atmospheric Aerosols*, edited by M. Kulmala and P. E. Wagner, pp. 759–769, Elsevier Sci., New York, 1996.

Penner, J. E., C. C. Chuang, and K. Grant, Climate forcing by carbonaceous and sulfate aerosols, *Clim. Dyn.*, *14*, 839–851, 1998.

Pham, M., J.-F. Muller, G. Brasseur, C. Granier, and G. Mégie, A three-dimensional study of the tropospheric sulfur cycle, *J. Geophys. Res.*, *100*, 26,061–26,092, 1995.

Pilinis, C., S. N. Pandis, and J. H. Seinfeld, Sensitivity of direct climate forcing by atmospheric aerosols to aerosol size and composition, *J. Geophys. Res.*, *100*, 18,739–18,754, 1995.

Pincus, R., and M. Baker, Precipitation, solar absorption, and albedo susceptibility in marine boundary layer clouds, *Nature*, *372*, 250–252, 1994.

Platnick, S., and S. Twomey, Determining the susceptibility of cloud albedo to changes in droplet concentration with the advanced very high resolution radiometer, *J. Appl. Meteorol.*, *33*, 334–347, 1994.

Podgorny, I. A., W. Conant, V. Ramanathan, and S. K. Satheesh, Aerosol modulation of atmospheric and surface solar heating over the tropical Indian Ocean, *Tellus, Ser. B*, *52*, 947–958, 2000.

Radke, L. F., J. A. Coakley, Jr., and M. D. King, Direct and remote sensing observations of the effects of ships on clouds, *Science*, *246*, 1146–1149, 1989.

Ramanathan, V., and J. A. Coakley, Climate modeling through radiative-convective models, *Rev. Geophys.*, *16*, 465–489, 1978.

Ramaswamy, V., and C.-T. Chen, Climate forcing-response relationships for greenhouse and shortwave radiative perturbations, *Geophys. Res. Lett.*, *24*, 667–670, 1997.

Reader, M. C., I. Fung, and N. McFarlane, The mineral dust aerosol cycle during the Last Glacial Maximum, *J. Geophys. Res.*, *104*, 9381–9398, 1999.

Remer, L. A., Y. J. Kaufman, B. N. Holben, A. M. Thompson, and D. McNamara, Biomass burning aerosol size distribution and modeled optical properties, *J. Geophys. Res.*, *103*, 31,879–31,891, 1998.

Remer, L. A., Y. J. Kaufman, D. Tanré, Z. Levin, and D. A. Chu, Principles in remote sensing of aerosol from MODIS over land and ocean, in *Proceedings of the ALPS99 International Conference, 18–22 January 1999, Méribel, France*, pp. WK1/O/05/1–4, Cent. Natl. des Etudes Spatiales, Toulouse, France, 1999.

Restad, K., I. Isaksen, and T. K. Berntsen, Global distribution of sulfate in the troposphere, A three-dimensional model study, *Atmos. Environ.*, *32*, 3593–3609, 1998.

Rodhe, H., R. J. Charlson, and T. L. Anderson, Avoiding circular logic in climate modeling, *Clim. Change*, *44*, 419–422, 2000.

Roelofs, G.-J., J. Lelieveld, and L. Ganzeveld, Simulation of global sulfate distribution and the influence on effective cloud drop radii with a coupled photochemistry-sulfur cycle model, *Tellus, Ser. B*, *50*, 224–242, 1998.

Rosenfeld, D., TRMM observed first direct evidence of smoke from forest fires inhibiting rainfall, *Geophys. Res. Lett.*, *26*, 3105–3108, 1999.

Rosenfeld, D., Suppression of rain and snow by urban and industrial air pollution, *Science*, *287*, 1793–1796, 2000.

Ross, J. L., P. V. Hobbs, and B. Holben, Radiative characteristics of regional hazes dominated by smoke from biomass burning in Brazil: Closure tests and direct radiative forcing, *J. Geophys. Res.*, *103*, 31,925–31,941, 1998.

Rotstayn, L., Indirect forcing by anthropogenic aerosols: A general circulation model calculation of the effective-radius

and cloud lifetime effects, *J. Geophys. Res.*, *104*, 9369–9380, 1999.

Russell, P. B., and J. Heintzenberg, An overview of the ACE-2 Clear Sky Column Closure Experiment (CLEARCOLUMN), *Tellus, Ser. B*, *52*, 463–483, 2000.

Russell, P. B., J. M. Livingston, P. Hignett, S. Kinne, J. Wong, A. Chien, R. Bergstrom, P. Durkee, and P. V. Hobbs, Aerosol-induced radiative flux changes off the United States mid-Atlantic coast: Comparison of values calculated from Sun-photometer and in situ data with those measured by airborne pyranometer, *J. Geophys. Res.*, *104*, 2289–2307, 1999.

Satheesh, S. K., V. Ramanathan, X. Li-Jones, J. M. Lobert, I. A. Podgorny, J. M. Prospero, B. N. Holben, and N. G. Loeb, A model for the natural and anthropogenic aerosols over the tropical Indian Ocean derived from Indian Ocean Experiment data, *J. Geophys. Res.*, *104*, 27,421–27,440, 1999.

Sausen, R., K. Gierens, M. Ponater, and U. Schumann, A diagnostic study of the global distribution of contrails, part I, Present-day climate, *Theor. Appl. Climatol.*, *61*, 127–141, 1998.

Schmid, B., et al., Clear-sky closure studies of lower tropospheric aerosol and water vapor during ACE-2 using airborne sunphotometer, airborne in situ, space-borne, and ground-based measurements, *Tellus, Ser. B*, 52, 568–593, 2000.

Schult, I., J. Feichter, and W. F. Cooke, Effect of black carbon and sulfate aerosols on the global radiation budget, *J. Geophys. Res.*, *102*, 30,107–30,117, 1997.

Schwartz, S. E., and A. Slingo, Enhanced shortwave cloud radiative forcing due to anthropogenic aerosols, in *Clouds, Chemistry, and Climate, Global Environ. Change*, vol. 35, edited by P. J. Crutzen and V. Ramanathan, *NATO ASI Ser. I*, pp. 191–235, Springer-Verlag, New York, 1995.

Shine, K. P., and P. M. de F. Forster, The effects of human activity on radiative forcing of climate change: A review of recent developments, *Global Planet. Change*, *20*, 205–225, 1999.

Shine, K. P., Y. Fouquart, V. Ramaswamy, S. Solomon, and J. Srinivasan, Radiative forcing of climate change, in *Climate Change 1995: The Science of Climate Change, The Contribution of Working Group I to the Second Assessment Report of the IPCC*, edited by J. T. Houghton et al., chap. 2.4, pp. 108–118, Cambridge Univ. Press, New York, 1996.

Smith, W. L., S. Ackerman, H. Revercomb, H. Huang, D. H. DeSlover, W. Feltz, L. Gumley, and A. Collard, Infrared spectral absorption of nearly invisible cirrus clouds, *Geophys. Res. Lett.*, *25*, 1137–1140, 1998.

Sokolik, I. N., and O. B. Toon, Direct radiative forcing by anthropogenic airborne mineral aerosols, *Nature*, *381*, 681–683, 1996.

Sokolik, I. N., and O. B. Toon, Incorporation of mineralogical composition into models of the radiative properties of mineral aerosol from UV to IR wavelengths, *J. Geophys. Res.*, *104*, 9423–9444, 1999.

Sokolik, I. N., A. Andronova, and T. C. Johnson, Complex refractive index of atmospheric dust aerosols, *Atmos. Environ., Part A*, *27*, 2495–2502, 1993.

Sokolik, I. N., O. B. Toon, and R. W. Bergstrom, Modeling the direct radiative characteristics of airborne mineral aerosols at infrared wavelengths, *J. Geophys. Res.*, *103*, 8813–8826, 1998.

Soufflet, V., D. Tanré, A. Royer, and N. T. O'Neill, Remote sensing of aerosols over boreal forest and lake water from AVHRR data, *Remote Sens. Environ.*, *60*, 22–34, 1997.

Ström, J., and S. Ohlsson, In situ measurements of enhanced crystal number densities in cirrus clouds caused by aircraft exhaust, *J. Geophys. Res.*, *103*, 11,355–11,361, 1998.

Swap, R., S. Ulanski, M. Cobbett, and M. Garstang, Temporal and spatial characteristics of Saharan dust outbreaks, *J. Geophys. Res.*, *101*, 4205–4220, 1996.

Tanré, D., Y. J. Kaufman, M. Herman, and S. Mattoo, Remote sensing of aerosol properties over oceans using the MODIS/EOS spectral radiances, *J. Geophys. Res.*, *102*, 16,971–16,988, 1997.

Tanré, D., L. A. Remer, Y. J. Kaufman, S. Mattoo, P. V. Hobbs, J. M. Livingston, P. B. Russell, and A. Smirnov, Retrieval of aerosol optical thickness and size distribution over ocean from the MODIS airborne simulator during TARFOX, *J. Geophys. Res.*, *104*, 2261–2278, 1999.

Taylor, J. P., and A. McHaffie, Measurements of cloud susceptibility, *J. Atmos. Sci.*, *51*, 1298–1306, 1994.

Tegen, I., and I. Fung, Contribution to the atmospheric mineral aerosol load from land surface modification, *J. Geophys. Res.*, *100*, 18,707–18,726, 1995.

Tegen, I., and A. Lacis, Modeling of particle size distribution and its influence on the radiative properties of mineral dust, *J. Geophys. Res.*, *101*, 19,237–19,244, 1996.

Tegen, I., A. Lacis, and I. Fung, The influence of mineral aerosols from disturbed soils on climate forcing, *Nature*, *380*, 419–422, 1996.

Tegen, I., P. Hollrigl, M. Chin, I. Fung, D. Jacob, and J. E. Penner, Contribution of different aerosol species to the global aerosol extinction optical thickness: Estimates from model results, *J. Geophys. Res.*, *102*, 23,895–23,915, 1997.

ten Brink, H. M., C. Kruisz, G. P. A. Kos, and A. Berner, Composition/size of the light-scattering aerosol in the Netherlands, *Atmos. Environ.*, *31*, 3955–3962, 1997.

Twohy, C. H., A. D. Clarke, S. G. Warren, L. F. Radke, and R. J. Charlson, Light-absorbing material extracted from cloud droplets and its effect on cloud albedo, *J. Geophys. Res.*, *94*, 8623–8631, 1989.

Twomey, S., Pollution and the planetary albedo, *Atmos. Environ.*, *8*, 1251–1256, 1974.

van Dorland, R., F. J. Dentener, and J. Lelieveld, Radiative forcing due to tropospheric ozone and sulfate aerosols, *J. Geophys. Res.*, *102*, 28,079–28,100, 1997.

Veefkind, J. P., J. C. H. van der Hage, and H. M. ten Brink, Nephelometer derived and directly measured aerosol optical depth of the atmospheric boundary layer, *Atmos. Res.*, *41*, 217–228, 1996.

Veefkind, J. P., G. de Leeuw, and P. A. Durkee, Retrieval of aerosol optical depth over land using two-angle view satellite radiometry during TARFOX, *Geophys. Res. Lett.*, *25*, 3135–3138, 1998.

Veefkind, J. P., G. de Leeuw, P. A. Durkee, P. B. Russell, P. V. Hobbs, and J. M. Livingston, Aerosol optical depth retrieval using ATSR-2 and AVHRR data during TARFOX, *J. Geophys. Res.*, *104*, 2253–2260, 1999.

von Hoyningen-Huene, W., K. Wenzel, and S. Schienbein, Radiative properties of desert dust and its effect on radiative balance, *J. Aerosol Sci.*, *30*, 489–502, 1999.

Wanner, W., A. H. Srahler, B. Hu, P. Lewis, J.-P. Muller, X. Li, C. L. Barker Schaaf, and M. J. Barnsley, Global retrieval of bidirectional reflectance and albedo over land from EOS MODIS and MISR data: Theory and algorithm, *J. Geophys. Res.*, *102*, 17,143–17,161, 1997.

Warren, S. G., C. J. Hahn, J. London, R. M. Chervin, and R. L. Jenne, Global distribution of total cloud cover and cloud type amounts over the ocean, *NCAR Tech. Note TN-317+STR*, 42 pp. + 170 maps, 1998.

West, J. J., C. Pilinis, A. Nenes, and S. N. Pandis, Marginal direct climate forcing by atmospheric aerosols, *Atmos. Environ.*, *32*, 2531–2542, 1998.

Wetzel, M., and L. L. Stowe, Satellite-observed patterns in stratus microphysics, aerosol optical thickness, and shortwave radiative forcing, *J. Geophys. Res.*, *104*, 31,287–31,299, 1999.

Wyser, K., and J. Ström, A possible change in cloud radiative forcing due to aircraft exhaust, *Geophys. Res. Lett.*, *25*, 1673–1676, 1998.

Yamasoe, M. A., Y. J. Kaufman, O. Dubovik, L. A. Remer, B. N. Holben, and P. Artaxo, Retrieval of the real part of the refractive index of smoke particles from Sun/sky measurements during SCAR-B, *J. Geophys. Res.*, *103*, 31,893–31,902, 1998.

O. Boucher, Laboratoire d'Optique Atmosphérique, UFR de Physique, Bâtiment P5, Université des Sciences et Technologies de Lille, 59655 Villeneuve d'Ascq Cedex, France. (boucher@loa.univ-lille1.fr)

J. Haywood, Meteorological Research Flight, U.K. Meteorological Office, DERA, Farnborough, Hampshire, GU14 0LX, England. (jmhaywood@meto.gov.uk)